

1 Evidence of high N₂ fixation rates in the temperate Northeast 2 Atlantic

3
4 Debany Fonseca-Batista^{1,2}, Xuefeng Li^{1,3}, Virginie Riou⁴, Valérie Michotey⁴, Florian Deman¹,
5 François Fripiat⁵, Sophie Guasco⁴, Natacha Brion¹, Nolwenn Lemaitre^{1,6,7}, Manon Tonnard^{6,8},
6 Morgane Gallinari⁶, Hélène Planquette⁶, Frédéric Planchon⁶, Géraldine Sarthou⁶, Marc Elskens¹,
7 Julie LaRoche², Lei Chou³, Frank Dehairs¹

8
9 ¹ Analytical, Environmental and Geo-Chemistry, Earth System Sciences Research Group, Vrije Universiteit Brussel,
10 1050 Brussels, Belgium

11 ² Department of Biology, Dalhousie University, Halifax, Nova Scotia, Canada B3H 4R2

12 ³ Service de Biogéochimie et Modélisation du Système Terre, Université Libre de Bruxelles, 1050 Brussels, Belgium

13 ⁴ Aix-Marseille Univ, Université de Toulon, CNRS, IRD, MIO, Marseille, France

14 ⁵ Max Planck Institute for Chemistry, Climate Geochemistry Department, 55128 Mainz, Germany

15 ⁶ Laboratoire des Sciences de l'Environnement MARin – CNRS UMR 6539 – Institut Universitaire Européen de la
16 Mer, 29280 Plouzané, France

17 ⁷ Department of Earth Sciences, Institute of Geochemistry and Petrology, ETH-Zürich, 8092 Zürich, Switzerland

18 ⁸ Institute for Marine and Antarctic Studies, University of Tasmania, Hobart, TAS 7001, Australia

19

20 Correspondence to: Debany Fonseca P. Batista (dbatista8@hotmail.com)

21 **Abstract.** Diazotrophic activity and primary production (PP) were investigated along two transects (Belgica
22 BG2014/14 and GEOVIDE cruises) off the western Iberian Margin and the Bay of Biscay in May 2014. Substantial
23 N₂ fixation activity was observed at 8 of the 10 stations sampled, ranging overall from 81 to 384 $\mu\text{mol N m}^{-2} \text{d}^{-1}$ (0.7
24 to 8.2 $\text{nmol N L}^{-1} \text{d}^{-1}$), with two sites close to the Iberian Margin situated between 38.8° N and 40.7° N yielding rates
25 reaching up to 1355 and 1533 $\mu\text{mol N m}^{-2} \text{d}^{-1}$. Primary production was relatively lower along the Iberian Margin with
26 rates ranging from 33 to 59 $\text{mmol C m}^{-2} \text{d}^{-1}$, while it increased towards the northwest away from the Peninsula,
27 reaching as high as 135 $\text{mmol C m}^{-2} \text{d}^{-1}$. In agreement with the area-averaged Chl *a* satellite data contemporaneous
28 with our study period, our results revealed that post-bloom conditions prevailed at most sites, while at the
29 northwesternmost station the bloom was still ongoing. When converted to carbon uptake using Redfield
30 stoichiometry, N₂ fixation could support 1 to 3% of daily PP in the euphotic layer at most sites, except at the two
31 most active sites where this contribution to daily PP could reach up to 25%. At the two sites where N₂ fixation
32 activity was the highest, the prymnesiophyte-symbiont *Candidatus Atelocyanobacterium thalassa* (UCYN-A)
33 dominated the *nifH* sequence pool, while the remaining recovered sequences belonged to non-cyanobacterial
34 phylotypes. At all the other sites however, the recovered *nifH* sequences were exclusively assigned phylogenetically
35 to non-cyanobacterial phylotypes. The intense N₂ fixation activities recorded at the time of our study were likely
36 promoted by the availability of phytoplankton-derived organic matter produced during the spring bloom, as
37 evidenced by the significant surface particulate organic carbon concentrations. Also, the presence of excess
38 phosphorus signature in surface waters seemed to contribute to sustaining N₂ fixation, particularly at the sites with
39 extreme activities. These results provide a mechanistic understanding of the unexpectedly high N₂ fixation in
40 productive waters of the temperate North Atlantic, and highlight the importance of N₂ fixation for future assessment
41 of global N inventory.

42

43 **1 Introduction**

44 Dinitrogen (N₂) fixation is the major pathway of nitrogen (N) input to the global ocean and thereby contributes to
45 sustaining oceanic primary productivity (Falkowski, 1997). The conversion by N₂-fixing micro-organisms
46 (diazotrophs) of dissolved N₂ gas into bioavailable nitrogen also contributes to new production in the euphotic layer
47 and as such, to the subsequent sequestration of atmospheric carbon dioxide into the deep ocean (Gruber, 2008).
48 Estimating the overall contribution of N₂ fixation to carbon sequestration in the ocean requires an assessment of the
49 global marine N₂ fixation.

50 Until recently most studies of N₂ fixation have focused on the tropical and subtropical regions of the global ocean,
51 with few attempts to measure N₂ fixation at higher latitudes, with the exception of enclosed brackish seas
52 (Ohlendieck et al., 2000; Luo et al., 2012; Farnelid et al., 2013). The intense research efforts in the low latitude
53 regions stem for the observable presence of cyanobacterial diazotrophs such as the diatom-diazotroph association
54 (DDA) and the colony-forming filamentous *Trichodesmium* (Capone, 1997; Capone et al., 2005; Foster et al., 2007).
55 *Trichodesmium* in particular, was long considered as the most active diazotroph in the global ocean. It has mostly
56 been reported in tropical and subtropical oligotrophic oceanic waters which are thought to represent the optimal
57 environment for its growth and N₂-fixing activity (Dore et al., 2002; Breitbarth et al., 2007; Montoya et al., 2007;
58 Needoba et al., 2007; Moore et al., 2009; Fernández et al., 2010; Snow et al., 2015). In low latitude regions, warm
59 stratified surface waters depleted in dissolved inorganic nitrogen (DIN), are assumed to give a competitive advantage
60 to diazotrophs over other phytoplankton since only they can draw N from the unlimited dissolved N₂ pool for their
61 biosynthesis. As such, past estimates of global annual N₂ fixation were mainly based on information gathered from
62 tropical and subtropical regions, while higher latitude areas have been poorly explored for diazotrophic activity (Luo
63 et al., 2012).

64 Studies using genetic approaches targeting the *nifH* gene encoding the nitrogenase enzyme, essential for diazotrophy,
65 have shown the presence of diverse diazotrophs throughout the world's oceans, extending their ecological niche
66 (Farnelid et al., 2011; Cabello et al., 2015; Langlois et al., 2015). Small diazotrophs such as unicellular diazotrophic
67 cyanobacteria (UCYN classified in groups A, B and C) and non-cyanobacterial diazotrophs, mostly heterotrophic
68 bacteria (e.g. Alpha- and Gammaproteobacteria), have been observed over a wide range of depths and latitudes,
69 thereby expanding the potential for diazotrophy to a much broader geographic scale (Langlois et al., 2005, 2008;
70 Krupke et al., 2014; Cabello et al., 2015). The discovery of a methodological bias associated to the commonly used
71 ¹⁵N₂ bubble-addition technique (Mohr et al., 2010) and the presence of an abundant diazotrophic community in high
72 latitude regions actively fixing N₂ (Needoba et al., 2007; Rees et al., 2009; Blais et al., 2012; Mulholland et al., 2012;
73 Shiozaki et al., 2015), indicate that more efforts are needed to better constrain oceanic N₂ fixation and diazotrophic
74 diversity at higher latitudes.

75 In the Northeast Atlantic, the large input of iron-rich Saharan dust alleviating dissolved iron (dFe) limitation of the
76 nitrogenase activity (Fe being a co-factor of the N₂-fixing enzyme) (Raven, 1988; Howard & Rees, 1996; Mills et al.,
77 2004; Snow et al., 2015) and the upwelling of subsurface waters with low DIN (dissolved inorganic nitrogen) to
78 phosphate ratios, make this region highly favorable for N₂ fixation activity (Deutsch et al., 2007; Moore et al., 2009).
79 In addition, the eastern North Atlantic has been observed to harbour a highly active and particularly diverse
80 diazotrophic community (Langlois et al., 2008; Moore et al., 2009; Großkopf et al., 2012; Ratten et al., 2015;
81 Fonseca-Batista et al., 2017) not only in the tropical and subtropical regions but also in the temperate Iberian region
82 which was reported to be a hotspot for the globally important prymnesiophyte-UCYN-A symbiotic associations
83 (Cabello et al., 2015). Earlier studies in the Iberian open waters investigated diazotrophic activity either under
84 stratified water column conditions of boreal summer and autumn (Moore et al., 2009; Benavides et al., 2011; Snow et

85 al., 2015; Fonseca-Batista et al., 2017) or during the winter convection period (Rijkenberg et al., 2011; Agawin et al.,
86 2014). Here, we present N₂ fixation rate measurements and the taxonomic affiliation of the diazotrophic community
87 from two consecutive campaigns carried out in the Northeast sector of the Atlantic Ocean in May 2014, during and
88 after the spring bloom.

89 **2 Material and Methods**

90 **2.1 Site description and sample collection**

91 Field experiments were conducted during two nearly simultaneous cruises in May 2014. The Belgica BG2014/14
92 cruise (21–30 May 2014, R/V *Belgica*), investigated the Bay of Biscay and the western Iberian Margin. In parallel,
93 the GEOVIDE expedition in the framework of the international GEOTRACES program (GA01 section, May 16 to
94 June 29 2014, R/V *Pourquoi pas?*) sailed from the Portuguese shelf area towards Greenland and ended in
95 Newfoundland, Canada (<http://dx.doi.org/10.17600/14000200>). N₂ fixation activities were determined at ten stations
96 within the Iberian Basin, among which four sites were investigated during the GEOVIDE cruise (stations Geo-1,
97 Geo-2, Geo-13 and Geo-21) and six sites during the BG2014/14 cruise (stations Bel-3, Bel-5, Bel-7, Bel-9, Bel-11
98 and Bel-13; Fig. 1).

99 All sampling sites were located within the Iberian Basin Portugal Current System (PCS) (Ambar and Fiúza, 1994)
100 which is influenced by highly fluctuating wind stresses (Frouin et al., 1990). The predominant upper layer water mass
101 in this basin is the Eastern North Atlantic Central Water (ENACW), a winter-mode water, which according to Fiúza
102 (1984) consists of two components (see θ/S diagrams in Supporting Information Fig. S1): (i) the lighter, relatively
103 warm (> 14 °C) and salty (salinity > 35.6) ENACW_{st} formed in the subtropical Azores Front region ($\sim 35^\circ$ N) when
104 Azores Mode Water is subducted as a result of strong evaporation and winter cooling; and (ii) the colder and less
105 saline ENACW_{sp}, underlying the ENACW_{st}, formed in the subpolar eastern North Atlantic (north of 43° N) through
106 winter cooling and deep convection (McCartney and Talley, 1982). The spatial distribution of these Central Waters
107 allowed the categorization of the sampling sites into 2 groups: (i) ENACW_{sp} stations north of 43° N (Bel-3, Bel-5,
108 Bel-7, and Geo-21) only affected by the ENACW_{sp} (Fig. S1a, b) and (ii) ENACW_{st} stations, south of 43° N,
109 characterized by an upper layer influenced by the ENACW_{st} and an subsurface layer, by the ENACW_{sp} (Fig. S1a,
110 b). Most of the ENACW_{st} stations were open ocean sites (Bel-9, Bel-11, Bel-13, and Geo-13) while two stations
111 were in proximity of the Iberian shelf (Geo-1 and Geo-2) (Tonnard et al., 2018).

112 Temperature, salinity and photosynthetically active radiation (PAR) profiles down to 1500 m depth were obtained
113 using a conductivity-temperature-depth (CTD) sensor (SBE 09 and SBE 911+, during the BG2014/14 and GEOVIDE
114 cruises, respectively) fitted to the rosette frames. For all biogeochemical measurements, seawater samples were
115 collected with Niskin bottles attached to the rosette and closed at specific depths in the upper 200 m. In particular, for
116 stable isotope incubation experiments seawater was collected in 4.5 L acid-cleaned polycarbonate (PC) bottles from
117 four depths corresponding to 54%, 13%, 3% and 0.2% of surface PAR at stations Bel-3, Bel-5, Bel-7, Bel-9, Bel-11,
118 and Geo-2. At stations Geo-1, Geo-13 and Geo-21, two additional depths corresponding to 25% and 1% of surface
119 PAR were also sampled for the same purpose.

120 **2.2 Nutrient measurements**

121 Ammonium (NH₄⁺) concentrations were measured on board during both cruises, while nitrate + nitrite (NO₃⁻ + NO₂⁻)
122 concentrations were measured on board only during the GEOVIDE expedition. During the BG2014/14 cruise,

123 samples for $\text{NO}_3^- + \text{NO}_2^-$ and phosphate (PO_4^{3-}) measurements were filtered (0.2 μm) and stored at -20°C until
124 analysis at the home-based laboratory. PO_4^{3-} data are not available for the GEOVIDE cruise.
125 Nutrient concentrations were determined using the conventional fluorometric (for NH_4^+) (Holmes et al., 1999) and
126 colorimetric methods (for the other nutrients) (Grasshoff et al., 1983) with detection limits (DL) of 64 nmol L^{-1}
127 (NH_4^+), 90 nmol L^{-1} ($\text{NO}_3^- + \text{NO}_2^-$) and 60 nmol L^{-1} (PO_4^{3-}). For the BG2014/14 cruise, chlorophyll *a* (Chl *a*)
128 concentrations were determined according to Yentsch and Menzel (1963). Briefly, 250 mL of seawater was filtered
129 onto Whatman GF/F glass microfiber filters (0.7 μm nominal pore size), followed by pigment extraction in 90%
130 acetone, centrifugation and fluorescence measurement using a Shimadzu RF-150 fluorometer. For the GEOVIDE
131 cruise, Chl *a* concentrations were measured as described in Ras et al. (2008). Briefly, filters samples were extracted
132 in 100% methanol, disrupted by sonification, and clarified by vacuum filtration through Whatman GF/F filters. The
133 extracts were analysed by high-performance liquid chromatography (HPLC Agilent Technologies 1200).

134 2.3 $^{15}\text{N}_2$ fixation and $^{13}\text{C}\text{-HCO}_3^-$ uptake rates

135 N_2 fixation and primary production (PP) were determined simultaneously from the same incubation sample at each
136 depth in duplicate, using the $^{15}\text{N}\text{-N}_2$ dissolution method (Großkopf et al., 2012) and $^{13}\text{C}\text{-NaHCO}_3$ tracer addition
137 technique (Hama et al., 1983), respectively. Details concerning the applied $^{15}\text{N}_2$ dissolution method can be found in
138 Fonseca-Batista et al. (2017). Briefly, $^{15}\text{N}_2$ -enriched seawater was prepared by degassing prefiltered (0.2 μm) low
139 nutrient seawater, under acid-clean conditions using a peristaltic pump slowly circulating (100 mL min^{-1}) the
140 seawater through two degassing membrane contactor systems (MiniModule, Liqui-Cel) in series, held under high
141 vacuum (50 mbar). The degassed water was directly transferred into 2 L gastight Tedlar bags (Sigma-Aldrich) fitted
142 with a septum through which 30 mL of pure $^{15}\text{N}_2$ gas (98 ^{15}N atom%, Eurisotop, lot number 23/051301) was injected
143 before the bags were shaken 24 hours for tracer equilibration. This $^{15}\text{N}_2$ gas batch was previously shown to be free of
144 ^{15}N -labelled contaminants such as nitrate, nitrite, ammonium and nitrous oxide (Fonseca-Batista et al., 2017). Each
145 PC incubation bottle was partially filled with sampled seawater, then amended with 250 mL of $^{15}\text{N}_2$ -enriched
146 seawater and spiked with 3 mL of ^{13}C -labelled dissolved inorganic carbon (DIC; 200 mmol L^{-1} solution of
147 $\text{NaH}^{13}\text{CO}_3$, 99%, Eurisotop). The ^{13}C -DIC added to a 4.5 L incubation bottle results in a $\sim 6.5\%$ increment of the
148 initial DIC content, considered equal to the average oceanic DIC concentration ($\sim 2000 \mu\text{mol kg}^{-1}$; Zeebe and Wolf-
149 Gladrow, 2003). This allows sufficient tracer enrichment for a sensitive detection in the particulate organic carbon
150 (POC) pool as a result of incorporation (Hama et al., 1983). Finally, each incubation bottle was topped off with the
151 original seawater sample. Samples were then incubated for 24 hours in on-deck incubators circulated with surface
152 seawater and wrapped with neutral density screens (Rosco) simulating the in situ irradiance conditions. After
153 incubation, water was transferred under helium pressure from each PC bottle into triplicate 12 mL gastight Exetainer
154 vials (Labco) poisoned (100 μL of saturated HgCl_2 solution) and pre-flushed with helium for the determination of the
155 ^{15}N and ^{13}C atom% enrichments of the dissolved N_2 (in duplicate) and DIC pools. The remaining incubated sample
156 was filtered onto pre-combusted MGF filters (glass microfiber filters, 0.7 μm nominal pore size, Sartorius), which
157 were subsequently dried at 60°C and stored at room temperature. The natural concentration and isotopic composition
158 of POC and particulate nitrogen (PN) were assessed by filtering immediately after sampling an additional 4.5 L of
159 non-spiked seawater from each depth. All samples were measured for POC and PN concentrations and isotopic
160 compositions using an elemental analyser (EuroVector Euro EA 3000) coupled to an isotope ratio mass spectrometer
161 (Delta V Plus, Thermo Scientific) and calibrated against international certified reference materials (CRM): IAEA-N1
162 and IAEA-305B for N and IAEA-CH6 and IAEA-309B for C. The isotopic composition of the DIC and dissolved N_2
163 pools was determined using a gas bench system coupled to an IRMS (Nu Instruments Perspective). Exetainers vials

164 were first injected with He to create a 4 mL headspace and then equilibrated on a rotatory shaker: for 12 hours after
 165 phosphoric acid addition (100 μ L, 99%, Sigma-Aldrich) for DIC analyses and only for an hour without acid addition
 166 for N_2 analyses. DIC measurements were corrected according to Miyajima et al. (1995) and $^{15}N_2$ enrichments were
 167 calibrated with atmospheric N_2 . N_2 fixation and carbon uptake volumetric rates were computed as shown in Equation
 168 1:

$$169 \quad N_2 \text{ or } HCO_3^- \text{ uptake rate (nmol } L^{-1}d^{-1} \text{ or } \mu\text{mol } m^{-3}d^{-1}) = \frac{A_{PN \text{ or } POC}^{final} - A_{PN \text{ or } POC}^{t=0}}{A_{N_2 \text{ or } DIC} - A_{PN \text{ or } POC}^{t=0}} \times \frac{[PN \text{ or } POC]}{\Delta t} \quad (1)$$

170 where $A_{PN \text{ or } POC}$ represents the ^{15}N or ^{13}C atom% excess of PN or POC, respectively, at the beginning ($t=0$) and end
 171 (final) of the incubation, while $A_{N_2 \text{ or } DIC}$ represents the ^{15}N or ^{13}C atom% excess of the dissolved inorganic pool (N_2
 172 or DIC); and Δt represents the incubation period.

173 Depth-integrated rates were calculated by non-uniform gridding trapezoidal integration for each station. The DL,
 174 defined as the minimal detectable uptake rates were determined as detailed in Fonseca-Batista et al. (2017). To do so,
 175 the minimal acceptable ^{15}N or ^{13}C enrichment of PN or POC after incubation (Montoya et al., 1996) is considered to
 176 be equal to the natural isotopic composition, specific to each sampled depth, plus three times the uncertainty obtained
 177 for N and C isotopic analysis of CRM. All remaining experiment-specific terms are then used to recalculate the
 178 minimum detectable uptake. Carbon uptake rates were always above their specific DL, while N_2 fixation was not
 179 detectable at any of the four depths of stations Bel-3 and Bel-5, nor at Bel-9 120 m, Bel-11 45 m and Geo-21 18 m
 180 (see Supporting Information Table S1).

181 **2.4 DNA sampling and *nifH* diversity analysis**

182 During the BG2014/14 and GEOVIDE cruises, water samples were also collected for DNA extraction and *nifH*
 183 sequencing at the stations where N_2 fixation rate measurements were carried out. Two liters of seawater samples were
 184 vacuum filtered (20 to 30 kPa) through sterile 0.2 μ m 47 mm membrane filters (cellulose acetate Sartorius type 111
 185 for BG2014/14; Millipore's Isopore - GTTP04700 for GEOVIDE) subsequently placed in cryovials directly flash
 186 deep frozen in liquid nitrogen. At the land-based laboratory samples were transferred to a $-80^\circ C$ freezer until nucleic
 187 acid extraction.

188 For the BG2014/14 samples, DNA was extracted from the samples using the Power Water DNA Isolation kit
 189 (MOBIO) and checked for integrity by agarose gel electrophoresis. The amplification of *nifH* sequences was
 190 performed on 3–50 ng μ L $^{-1}$ environmental DNA samples using one unit of Taq polymerase (5PRIME), by nested
 191 PCR according to Zani et al. (2000) and Langlois et al. (2005). Amplicons of the predicted 359-bp size observed by
 192 gel electrophoresis were cloned using the PGEM T Easy cloning kit (PROMEGA) according to the manufacturer's
 193 instructions. A total of 103 clones were sequenced by the Sanger technique (GATC, Marseille).

194 For the GEOVIDE samples, DNA was extracted using the QIAGEN DNeasy Plant Mini Kit as instructed by the
 195 manufacture, with a modified step to improve cell lysis. This step consisted of an incubation at $52^\circ C$ on an orbital
 196 shaker for 1 hour (300 rpm) with 50 μ L of lysozyme solution (5 mg mL $^{-1}$ in TE buffer), 45 μ L of Proteinase K
 197 solution (20 mg mL $^{-1}$ in MilliQ PCR grade water) and 400 μ L of AP1 lysis buffer from the QIAGEN DNeasy Plant
 198 Mini Kit. DNA concentration and purity were assessed with NanoDrop 2000 and then stored at $-80^\circ C$. The DNA
 199 samples were screened for the presence of the *nifH* gene as described in Langlois et al. (2005). Samples that tested
 200 positive were further prepared for next generation sequencing on an Illumina MiSeq platform using primers that
 201 included the *nifH*1/2 primers (Langlois et al., 2005; Ratten, 2017) attached to Illumina adaptors and barcodes for
 202 multiplexing in the Illumina MiSeq instrument. Next generation sequencing was carried out at the Integrated
 203 Microbiome Resource (IMR) of the Centre for Comparative and Evolutionary Biology (CGEB) at Dalhousie

204 University (Halifax, Canada). Raw Illumina paired-end reads of *nifH* were preprocessed using the QIIME pipeline
205 (Quantitative Insights Into Microbial Ecology; Caporaso et al., 2010) following the IMR workflow
206 (https://github.com/mlangill/microbiome_helper/wiki/16S-standard-operating-procedure; Comeau et al., 2017). The
207 28 OTUs for the *nifH* genes presented in this study were assembled based on 96% identity of sequence reads.
208 DNA alignments were performed using the Molecular Evolutionary Genetics Analysis software (MEGA 7.0) (Kumar
209 et al., 2016) and *nifH* operational taxonomic units (*nifH*-OTUs) were defined with a maximum 5% divergence cut-
210 off. DNA sequences were translated into amino acid sequences, then *nifH* evolutionary distances considered as the
211 number of amino acid substitutions per site, were computed using the Poisson correction method (Nei, 1987). All
212 positions containing gaps and missing data were eliminated (see phylogenetic tree in Fig. 6). One representative
213 sequence of each *nifH*-OTU was deposited in GenBank under the accession numbers referenced from KY579322 to
214 KY579337, for the Belgica DNA samples and referenced from MH974781 to MH974795 for the GEOVIDE Iberian
215 samples.

216 **2.5 Statistical analysis**

217 The relationship between N₂ fixation activities and ambient physical and chemical properties was examined, using
218 SigmaPlot (Systat Software, San Jose, CA) by computing Spearman rank correlation coefficients linking depth-
219 integrated rates and volumetric rates of N₂ fixation and primary production to environmental variables. These
220 ambient variables were either averaged or integrated over the euphotic layer, or considered as discrete measurements.
221 These variables include temperature, salinity, Chl *a*, NH₄⁺, NO₃⁻+NO₂⁻, phosphorus excess (P* = [PO₄³⁻] - [NO₃⁻
222 +NO₂⁻] / 16) derived from in situ nutrient measurements and climatological data (Garcia et al., 2013), dissolved iron
223 concentrations determined for the GEOVIDE cruise (Tonnard et al., 2018) and satellite-derived dust deposition fluxes
224 at the time of our study (Giovanni online data system). When nutrient concentrations were below the DL we used the
225 DL value to run the correlation test. In addition, we ran a principal component analysis (PCA) using XLSTAT 2017
226 (Addinsoft, Paris, France, 2017) to get an overview of the interconnection between all the latter key variables with N₂
227 fixation at the time of our study. The output of the PCA are discussed in section 4.3.

228 **3 Results**

229 **3.1 Ambient environmental settings**

230 Surface waters of all the ENACWst stations showed a relatively strong stratification resulting from the progressive
231 spring heating, with sea surface temperature (SST) ranging from 15.3 (Geo-13) to 17.2 °C (Bel-13). At the surface,
232 nutrients were depleted (NO₃⁻ + NO₂⁻ < 0.09 μM in the upper 20 m; Fig. 2c, f) and Chl *a* concentrations were low (<
233 0.25 μg L⁻¹; Fig. 2a, d) but showed a subsurface maximum (between 0.5 and 0.75 μg L⁻¹ at approximately 50 m), a
234 common feature for oligotrophic open ocean waters. Amongst the ENACWst stations, station Geo-13 had a slightly
235 higher nutrient content (NO₃⁻ + NO₂⁻ = 0.7 μM) in the lower mixed layer depth (MLD) and a higher Chl *a*
236 concentration (> 0.5 μg L⁻¹ in the upper 35 m).

237 Surface waters at ENACWsp stations were less stratified (SST between 14.0 and 14.5 °C), were nutrient replete
238 (surface NO₃⁻ + NO₂⁻ ranging from 0.3 to 0.8 μM) and had a higher phytoplankton biomass (Chl *a* between 0.7 to 1.2
239 μg L⁻¹ in the upper 30 m except for station Bel-5). Highest Chl *a* values were observed at station Bel-7 (44.6° N, 9.3°
240 W), which appeared to be located within an anticyclonic mesoscale eddy as evidenced by the downwelling structure
241 detected in the Chl *a* and NO₃⁻ + NO₂⁻ profiles (Fig. 2a, c) at this location (as well as T and S sections, data not
242 shown).

243 3.2 Primary production and satellite-based Chl *a* observations

244 Primary production (PP), estimated through the incorporation of enriched bicarbonate ($^{13}\text{C-NaHCO}_3$) into the POC
245 pool, illustrated volumetric rates ranging from 7 to 3500 $\mu\text{mol C m}^{-3} \text{d}^{-1}$ (see Supporting Information Table S1) and
246 euphotic layer integrated rates ranging from 32 to 137 $\text{mmol C m}^{-2} \text{d}^{-1}$ (Fig. 3a, b, and Supporting Information Table
247 S2). PP was relatively homogenous in the Bay of Biscay (stations Bel-3, Bel-5 and Bel-7) and along the Iberian
248 Margin (Bel-9, Bel-11, Bel-13 and Geo-1) with average rates ranging from 33 to 43 $\text{mmol C m}^{-2} \text{d}^{-1}$, except for
249 station Bel-7 where it was slightly higher (52 $\text{mmol C m}^{-2} \text{d}^{-1}$; Fig. 3a, b, and Table S2), likely due to the presence of
250 an anticyclonic mesoscale structure at this location. PP increased westwards away from the Iberian Peninsula,
251 reaching highest values at stations Geo-13 and Geo-21 (79 and 135 $\text{mmol C m}^{-2} \text{d}^{-1}$, respectively; Fig. 3b), but also
252 slightly higher on the Portuguese shelf (reaching 59 $\text{mmol C m}^{-2} \text{d}^{-1}$ at Geo-2). These results are in the range of past
253 measurements in this region for the same period of the year, ranging from 19 to 103 $\text{mmol C m}^{-2} \text{d}^{-1}$ (Marañón et al.,
254 2000; Fernández et al., 2005; Poulton et al., 2006; Fonseca-Batista et al., 2017). Area-averaged Chl *a* derived from
255 satellite imagery for a time-period overlapping with ours (Giovanni online data system; Fig. 4a, b) revealed that post-
256 bloom conditions prevailed at most sites (Bel-3 to Bel-13 and Geo-1 to Geo-13) while bloom conditions were still
257 ongoing at station Geo-21 at the time of our study.

258 3.3 N_2 fixation and dominant diazotrophs at the sampling sites

259 Volumetric N_2 fixation rates were above the DL at 8 of the 10 stations sampled in this study (Bel-3 and Bel-5 being
260 below the DL) and ranged from 0.7 to 65.4 $\text{nmol N L}^{-1} \text{d}^{-1}$ (see Table S1), with areal rates ranging between 81 and
261 1533 $\mu\text{mol N m}^{-2} \text{d}^{-1}$ (Fig. 3c, d, and Table S2).

262 We observed intense N_2 fixation activities at the two sites (Bel-11 and Bel-13) most affected by ENACWst (Fig. S1).
263 At stations Bel-11 and Bel-13, volumetric rates of N_2 fixation ranged from 2.4 to 65.4 $\text{nmol N L}^{-1} \text{d}^{-1}$, with highest
264 rates found at surface level (65.4 and 45.0 $\text{nmol N L}^{-1} \text{d}^{-1}$, respectively), while areal rates averaged 1533 and 1355
265 $\mu\text{mol N m}^{-2} \text{d}^{-1}$, respectively. N_2 fixation was detected at all four GEOVIDE stations. Shelf-influenced (Geo-1 and
266 Geo-2) and open ocean (Geo-13) ENACWst sites, geographically close to Bel-11 and Bel-13, also displayed high N_2
267 fixation activities with volumetric rates ranging from 1.0 to 7.1 $\text{nmol N L}^{-1} \text{d}^{-1}$ (Table S1) while depth-integrated rates
268 averaged 141, 262 and 384 $\mu\text{mol N m}^{-2} \text{d}^{-1}$, respectively (Fig. 3c, d, and Table S2). Significant N_2 fixation rates were
269 also measured at stations that exhibited the highest primary production rates, including Bel-7, Geo-13 and Geo-21
270 (Fig. 3). We computed the relative contribution of N_2 fixation to PP by converting N_2 fixation rates to carbon uptake
271 using either the Redfield ratio of 6.6 or the determined median POC/PN ratio for natural particles (equivalent to the
272 mean value of 6.3 ± 1.1 , $\pm \text{SD}$, $n = 46$; Table 1). N_2 fixation contributed to less than 2% of PP at the ENACWsp sites
273 Bel-7 and Geo-21 and between 3 to 28% of PP at the ENACWst sites, except for station Bel-9 where it supported
274 about 1% of PP.

275 Screening of the *nifH* genes from DNA samples collected during the BG2014/14 cruise, returned positive *nifH*
276 presence at stations Bel-11 and Bel-13 that displayed the largest areal N_2 fixation rates. Cloning of the *nifH*
277 amplicons found in surface waters (54% PAR level where volumetric rates of N_2 fixation were the highest) yielded
278 103 *nifH* sequences. No successful *nifH* amplifications were obtained at the other Belgica stations or depths where
279 diazotrophic activities were lower or undetectable. All the clones ($n = 41$) recovered from station Bel-11 were
280 taxonomically assigned to a single OTU that had 99% identity at the nucleotide level and 100% similarity at the
281 amino acid level with the symbiotic diazotrophic cyanobacteria UCYN-A1 or *Candidatus Atelocyanobacterium*
282 *thalassa*, first characterized from station ALOHA in the North Pacific (Fig. 5a and 6) (Thompson et al., 2012). While
283 the UCYN-A OTU also dominated the clones recovered from station Bel-13, fourteen additional *nifH* phylotypes

284 affiliated with non-cyanobacterial diazotrophs were also recovered at that station (Fig. 5a and 6). Among these 15
285 OTUs, represented by a total of 62 sequenced clones, 45.2% of the sequences were affiliated to UCYN-A1 (identical
286 to those found at Bel-11), and the rest to heterotrophic bacteria with 25.8% affiliated to Bacteroidetes, 19.3% to
287 Firmicutes and 9.7% to Proteobacteria (Gamma-, Epsilon- and Delta-proteobacteria; Fig. 5a and 6). For the
288 GEOVIDE cruise, *nifH* screening returned positive *nifH* presence at stations Geo-2, Geo-13 and Geo-21. Next
289 generation sequencing of these amplicons yielded in total 21001 reads, with a range of 170 to 9239 *nifH* amplicons
290 per sample, belonging exclusively to non-cyanobacterial diazotrophs, with the major affiliation to Verrucomicrobia,
291 and Gamma-, Delta- and Alpha-proteobacteria, representing 54, 28, 15 and 1% of total *nifH* amplicons, respectively
292 (Fig. 5b and 6). Members of a clade that has recently been characterized from the TARA expedition through
293 metagenome assembled genomes of marine heterotrophic diazotrophs (Delmont et al., 2018), were found among the
294 Gammaproteobacteria OTU types that dominated the community at station Geo-21.

295 **3.4 Relationship between N₂ fixation rates and environmental variables**

296 N₂ fixation activities were measured in surface waters characterized by relatively low SST (12.5–17.3 °C) and a wide
297 range of dissolved inorganic nitrogen (DIN) concentrations (NO₃⁻ + NO₂⁻ from < 0.1 to 7.6 μM). Water column
298 integrated N₂ fixation tended to increase with average surface water salinity (n = 10, *p* < 0.05, Table S3) but was
299 inversely correlated to satellite-based dust deposition in May 2014, the month during which our sampling took place
300 (n = 10, *p* < 0.01). Volumetric rates of N₂ fixation tended to increase with temperature (n = 46, *p* < 0.01, Table S4)
301 and excess phosphorus concentration (only available for Belgica studied sites, n = 24, *p* < 0.01) while being
302 negatively correlated to nitrate plus nitrite concentration (n = 46, *p* < 0.01).

303 **4 Discussion**

304 During two quasi-simultaneous expeditions to the Iberian Basin and the Bay of Biscay in May 2014 (38.8–46.5° N),
305 we observed N₂ fixation activity in surface waters of most visited stations (except for the two northernmost sites in
306 the Bay of Biscay). Our results are in support of other recent studies that have observed diazotrophic communities
307 and significant N₂ fixation rates in marine environments departing from the previously established belief that
308 diazotrophs are preferentially associated with warm oceanic water and low fixed-nitrogen concentrations (Needoba et
309 al., 2007; Rees et al., 2009; Blais et al., 2012; Mulholland et al., 2012; Shiozaki et al., 2015). Although there is
310 growing evidence that diazotrophs and their activity can extend geographically to temperate coastal and shelf-
311 influenced regions, there still exist very few rate measurements at higher latitudes, especially in open waters. In the
312 following sections we shall (1) discuss the significance of N₂ fixation in the Iberian Basin as well as its relation to
313 primary productivity pattern and extend our view to the whole Atlantic Ocean, (2) provide information on the
314 taxonomic affiliation of diazotrophs present at the time of our study, and (3) explore potential environmental
315 conditions that may have supported this unexpectedly high diazotrophic activity in the Iberian Basin.

316 **4.1 Significance of N₂ fixation in the temperate ocean**

317 In the present study, we found surprisingly high N₂ fixation activities at most of the studied sites. Rates were
318 exceptionally elevated at two open ocean stations located between 38.8 and 40.7° N at about 11° W (averaging 1533
319 and 1355 μmol N m⁻² d⁻¹ at stations Bel-11 and Bel-13, respectively; Fig. 3c, d, and Tables S1 and S2). Although N₂
320 fixation was not detected in the central Bay of Biscay (stations Bel-3 and Bel-5), rates recorded at all the other sites
321 were relatively high, not only in shelf-influenced areas (141 and 262 μmol N m⁻² d⁻¹ at stations Geo-1 and Geo-2,

322 respectively) but also in the open ocean (average activities between 81 and 384 $\mu\text{mol N m}^{-2} \text{d}^{-1}$ at stations Bel-7, Bel-
323 9, Geo-13 and Geo-21).

324 By fuelling the bioavailable nitrogen pool, N_2 fixation may support marine primary production (PP), but the extent of
325 this contribution needs to be established for areas outside tropical and subtropical regions. PP rates measured here are
326 of similar range if not slightly higher than those reported in earlier investigations in the Northeast Atlantic from
327 subtropical to temperate waters (32 to 137 $\text{mmol C m}^{-2} \text{d}^{-1}$ relative to 19 to 103 $\text{mmol C m}^{-2} \text{d}^{-1}$) (Marañón et al.,
328 2000; Fernández et al., 2005; Poulton et al., 2006; Fonseca-Batista et al., 2017). However, the contribution of N_2
329 fixation to PP in the present work (1–28% of PP) reached values twice as high as those reported in other studies for
330 the tropical and subtropical northeast Atlantic (contributions to PP ranging from < 1% to 12%) (Voss et al., 2004;
331 Rijkenberg et al., 2011; Fonseca-Batista et al., 2017). This observation further questions the accepted premise that
332 oligotrophic surface waters of tropical and subtropical regions are the key environment where diazotrophic activity
333 significantly supports marine primary productivity (Capone et al., 2005; Luo et al., 2014). Nevertheless, it is
334 important to keep in mind that our computation relies on the assumption that only photoautotrophic diazotrophs
335 contribute to bulk N_2 fixation, which may not always be the case, particularly in the present study, where mostly
336 heterotrophic diazotrophs were observed. However, it is likely that all the recently fixed-nitrogen ultimately becomes
337 available for the whole marine autotrophic community.

338 Previous studies in the open waters of the Iberian Basin (35–50° N, east of 25° W) reported relatively lower N_2
339 fixation rates (from < 0.1 to 140 $\mu\text{mol N m}^{-2} \text{d}^{-1}$), regardless of whether the bubble-addition method (Montoya et al.,
340 1996) or the dissolution method (Mohr et al., 2010; Großkopf et al., 2012) was used. However, these studies were
341 carried out largely outside the bloom period, either during the late growing season (summer and autumn) (Moore et
342 al., 2009; Benavides et al., 2011; Snow et al., 2015; Riou et al., 2016; Fonseca-Batista et al., 2017) or during winter
343 (Rijkenberg et al., 2011; Agawin et al., 2014). In contrast, the present study took place in spring, during or just at the
344 end of the vernal phytoplankton bloom. Differences in timing of these various studies and to a lesser extent, in
345 methodologies (bubble-addition versus dissolution method) may explain the discrepancies in diazotrophic activity
346 observed between our study and earlier works. Yet, the 20 months survey by Moreira-Coello et al. (2017) in nitrogen-
347 rich temperate coastal waters in the southern Bay of Biscay, covering the seasonal spring bloom and upwelling
348 pulses, did not reveal significant N_2 fixation activities: from 0.1 to 1.6 $\mu\text{mol N m}^{-2} \text{d}^{-1}$ (up to 3 orders of magnitude
349 lower than those reported here). However, unlike our study, this work was carried out not only using the bubble-
350 addition method but also in an inner coastal system, as opposed to the mainly open waters investigated here, making
351 it difficult to predict which variable or combination of variables caused the difference observed between the two
352 studies.

353 Our maximal values recorded at stations Bel-11 and Bel-13 are one order of magnitude higher than maximal N_2
354 fixation rates reported further south for the eastern tropical and subtropical North Atlantic (reaching up to 360–424
355 $\mu\text{mol N m}^{-2} \text{d}^{-1}$) (Großkopf et al., 2012; Subramaniam et al., 2013; Fonseca-Batista et al., 2017). Besides these two
356 highly active sites, N_2 fixation rates at the other studied locations (ranging between 81 and 384 $\mu\text{mol N m}^{-2} \text{d}^{-1}$) were
357 still in the upper range of values reported for the whole eastern Atlantic region. Yet, conditions favouring N_2 fixation
358 are commonly believed to be met in tropical and subtropical regions where highest activities have mostly been
359 measured, particularly in the eastern North Atlantic (e.g., higher seawater temperature, DIN limiting concentrations,
360 excess phosphorus supply through eastern boundary upwelling systems) (Capone et al., 2005; Deutsch et al., 2007;
361 Luo et al., 2014; Fonseca-Batista et al., 2017).

362 In the Atlantic Ocean, very high N_2 fixation rates up to ~1000 $\mu\text{mol N m}^{-2} \text{d}^{-1}$ as observed here, have only been
363 reported for temperate coastal waters of the Northwest Atlantic (up to 838 $\mu\text{mol N m}^{-2} \text{d}^{-1}$) (Mulholland et al., 2012)

364 and for tropical shelf-influenced and mesohaline waters of the Caribbean and Amazon River plume (maximal rates
365 ranging between 898 and 1600 $\mu\text{mol N m}^{-2} \text{d}^{-1}$) (Capone et al., 2005; Montoya et al., 2007; Subramaniam et al.,
366 2008). Shelf and mesohaline areas have indeed been shown to harbour considerable N_2 fixation activity, not only in
367 tropical regions (Montoya et al., 2007; Subramaniam et al. 2008) but also in waters extending from temperate to polar
368 areas (Rees et al., 2009; Blais et al., 2012; Mulholland et al., 2012; Shiozaki et al., 2015). Yet, the environmental
369 conditions leading to the high N_2 fixation rates in these regions are currently not well understood. For tropical
370 mesohaline systems, the conditions proposed to drive such an intense diazotrophic activity include the occurrence of
371 highly competitive diatom-diazotrophs associations and the influence of excess phosphorus input (i.e., excess relative
372 to the canonical Redfield P/N ratio; expressed as P^*) from the Amazon River (Subramaniam et al., 2008). However,
373 such conditions of excess P were not observed in previous studies carried out in high latitude shelf regions with
374 elevated N_2 fixation activities (Blais et al., 2012; Mulholland et al., 2012; Shiozaki et al., 2015), nor was it distinctly
375 apparent in the present study (see section 4.3). In addition, while tropical mesohaline regions are characterized by the
376 predominance of diatom-diazotroph associations (and filamentous *Trichodesmium* spp.), in temperate shelf areas the
377 diazotrophic community is reported to be essentially dominated by UCYN-A and heterotrophic bacteria (Rees et al.,
378 2009; Blais et al., 2012; Mulholland et al., 2012; Agawin et al., 2014; Shiozaki et al., 2015; Moreira-Coello et al.,
379 2017).

380 **4.2 Features of the diazotrophic community composition in the temperate North Atlantic**

381 Our qualitative assessment of *nifH* diversity revealed a predominance of UCYN-A symbionts, only at the two stations
382 with the highest surface N_2 fixation rates (up to 65.4 and 45.0 $\text{nmol N L}^{-1} \text{d}^{-1}$ at Bel-11 and Bel-13, respectively;
383 Table S1) while the remaining *nifH* sequences recovered belonged to heterotrophic diazotrophs, at Bel-13 as well as
384 at all the other sites where *nifH* genes could be detected. No *Trichodesmium nifH* sequences were recovered from
385 either BG2014/14 or GEOVIDE DNA samples, and the absence of the filamentous cyanobacteria was also confirmed
386 by the CHEMTAX analysis of phytoplankton pigments (M. Tonnard, personal communication, January 2018).
387 Previous work in temperate regions of the global ocean, including the Iberian Margin also reported that highest N_2
388 fixation activities were predominantly related to the presence of UCYN-A symbionts, followed by heterotrophic
389 bacteria, while *Trichodesmium* filaments were low or undetectable (Needoba et al., 2007; Rees et al., 2009;
390 Mulholland et al., 2012; Agawin et al., 2014; Shiozaki et al., 2015; Moreira-Coello et al., 2017).

391 UCYN-A (in particular from the UCYN-A1 clade) were shown to live in symbioses with single-celled
392 prymnesiophyte algae (Thompson et al., 2012). This symbiotic association, considered obligate, has been reported to
393 be particularly abundant in the central and eastern basin of the North Atlantic (Rees et al., 2009; Krupke et al., 2014;
394 Cabello et al., 2015; Martínez-Pérez et al., 2016).

395 Besides UCYN-A, all the remaining *nifH* sequences recovered from both cruises, although obtained through different
396 approaches, belonged to non-cyanobacterial diazotrophs. The phylogenetic tree (Fig. 6) showed that the non-
397 cyanobacterial diazotrophs clustered with (1) Verrucomicrobia, a phylum yet poorly known that includes aerobic to
398 microaerophilic methanotrophs groups, found in a variety of environments (Khadem et al., 2010; Wertz et al., 2012),
399 (2) anaerobic bacteria, obligate or facultative, mostly affiliated to Cluster III phylotypes of functional nitrogenase
400 (e.g., Bacteroidetes, Firmicutes, Proteobacteria) and lastly (3) phylotypes from Clusters I, II, and IV (e.g.,
401 Proteobacteria and Firmicutes). Among the Cluster III phylotypes, Bacteroidetes are commonly encountered in the
402 marine environment and are known as specialized degraders of organic matter that preferably grow attached to
403 particles or algal cells (Fernández-Gómez et al., 2013). N_2 fixation activity has previously been reported in five
404 Bacteroidetes strains including *Bacteroides graminisolvens*, *Paludibacter propionicigenes* and *Dysgonomonas gadei*

405 (Inoue et al., 2015) which are the closest cultured relatives of the *nifH*-OTUs detected at station Bel-13 (Fig. 6).
406 Anaerobic Cluster III phylotypes have been previously recovered from different ocean basins (Church et al., 2005;
407 Langlois et al., 2005, 2008; Man-Aharonovich et al., 2007; Rees et al., 2009; Halm et al., 2012; Mulholland et al.,
408 2012). These diazotrophs were suggested to benefit from anoxic microzones found within marine snow particles or
409 zooplankton guts to fix N₂ thereby avoiding oxygenic inhibition of their nitrogenase enzyme (Braun et al., 1999;
410 Church et al., 2005; Scavotto et al., 2015). Therefore, the bloom to early post-bloom conditions, prevailing during our
411 study, were likely beneficial for the development of diazotrophic groups that depend on the availability of detrital
412 organic matter or on the association with grazing zooplankton. In contrast, at the northernmost Geo-21 station, we
413 observed a dominance of Gammaproteobacteria phylotypes belonging to a recently identified clade of marine
414 diazotrophs within the Oceanospirillales (Delmont et al., 2018).
415 These observations tend to strengthen the idea that not only UCYN-A (Cabello et al., 2015; Martínez-Pérez et al.,
416 2016) but also non-cyanobacterial diazotrophs (Halm et al., 2012; Shiozaki et al., 2014; Langlois et al., 2015) play a
417 substantial role in oceanic N₂ fixation. Although it is possible to assign a broad taxonomic affiliation to classify the
418 *nifH* genes, very little is known with respect to their physiology, their role in the ecosystem and the factors
419 controlling their distribution, due to the lack of representative whole genome sequences and environmentally relevant
420 strains available for experimentation (Bombar et al., 2016). While the widespread distribution of UCYN-A and non-
421 cyanobacterial diazotrophs has been reported, their contribution to in situ activity remains poorly quantified.

422 **4.3 Key environmental drivers of N₂ fixation**

423 Environmental conditions that promote autotrophic and heterotrophic N₂ fixation activity in the ocean are currently
424 not well understood (Luo et al., 2014). While heterotrophic diazotrophs would not be directly affected by the
425 commonly recognized environmental controls of autotrophic diazotrophy such as solar radiation, seawater
426 temperature and DIN, as they possess fundamentally different ecologies, the molecular and cellular processes for
427 sustaining N₂ fixation activity would nevertheless require a supply of dFe and P (Raven, 1988; Howard & Rees,
428 1996; Mills et al., 2004; Snow et al., 2015). Besides the need for these critical inorganic nutrients, heterotrophic N₂
429 fixation was also recently shown to be highly dependent on the availability of organic matter (Bonnet et al., 2013;
430 Rahav et al., 2013, 2016; Loescher et al., 2014).

431 Findings from the GEOVIDE cruise tend to support the hypothesis of a stimulating effect of organic matter
432 availability on N₂ fixation activity at the time of our study. Lemaitre et al. (2018) report that surface waters (upper
433 100–120 m) of the Iberian Basin (stations Geo-1 and Geo-13) and the West European Basin (Geo-21) carried
434 significant POC loads (POC of 166, 171 and 411 mmol C m⁻², respectively) with a dominant fraction of small size
435 POC (the 1–53 μm size fraction; 75%, 92% and 64% of the total POC, respectively). Smaller cells, usually being
436 slow-sinking particles, are more easily remineralized in surface waters (Villa-Alfageme et al., 2016). This is
437 confirmed by the very low export efficiency (only 3 to 4% of euphotic layer integrated PP) observed at stations Geo-
438 13 and Geo-21, suggesting an efficient shallow remineralisation (Lemaitre et al., 2018). This availability of organic
439 matter in the upper layers likely contributed to supplying remineralized P (organic P being generally more labile than
440 other organic nutrients; Vidal et al., 1999, 2003) and to enhancing the residence time of dFe originating from
441 atmospheric deposition due to the formation of organic ligands (Jickells, 1999; de Baar and de Jong, 2001; Sarthou et
442 al., 2003).

443 P* values from the BG2014/14 cruise (Table S1) and the climatological P* data for the Iberian Basin (Garcia et al.,
444 2013) do not exhibit a clear PO₄³⁻ excess in the region (P* ranging from -0.1 to 0.1 μmol L⁻¹; Fig. 1 and Tables S1
445 and S2). Nevertheless, Spearman rank correlations indicate that volumetric N₂ fixation rates were significantly

446 correlated with the BG2014/14 shipboard P* values ($n = 24$, $p < 0.01$, Table S4), with stations Bel-11 and Bel-13
447 weighing heavily in this correlation. Without the data from these two sites (data not shown), the correlation between
448 in situ P* and N₂ fixation rates is no longer significant ($n = 16$, $p = 0.163$), while P* becomes highly correlated with
449 PP and Chl *a* ($n = 16$, $p = 0.0257$ and 0.016 , respectively). This suggests that the effect of P* on N₂ fixation, although
450 not clearly evident from absolute values, was most important at stations Bel-11 and Bel-13 but nonetheless existent at
451 the other sites (Bel-7 and Bel-9). The occurrence of N₂ fixation in oligotrophic waters displaying weak P* values,
452 depleted in DIN and PO₄³⁻ but replete in dFe might in fact reflect the direct use by diazotrophs of dissolved organic
453 phosphorus (DOP). Indeed, according to Landolfi et al. (2015) diazotrophy ensures the supply of additional N and
454 energy for the enzymatic mineralization of DOP (synthesis of extracellular alkaline phosphatase). Therefore, a likely
455 enhanced DOP release towards the end of the spring bloom may have contributed to sustaining N₂ fixation in the
456 studied region. Such DOP utilization has indeed been reported for various marine organisms, particularly
457 diazotrophic cyanobacteria (Dyhrman et al., 2006; Dyhrman & Haley, 2006) and bacterial communities (Luo et al.,
458 2009).

459 Supply routes of dFe to surface waters of the investigated area relied on lateral advection from the continental shelf
460 (stations Geo-1 and Geo-2) (Tonnard et al., 2018), vertical mixing due to post-winter convection (Thuróczy et al.,
461 2010; Rijkenberg et al., 2012; García-Ibáñez et al., 2015), and/or atmospheric dust deposition (dry + wet).
462 Atmospheric deposition may have been particularly important for the area of stations Bel-11 and Bel-13 receiving
463 warm and saline surface waters from the subtropics.

464 Atmospheric aerosol deposition determined during the GEOVIDE cruise (Shelley et al., 2017), as well as the
465 satellite-based dust deposition (dry + wet) averaged over the month of May 2014 (Fig. S3b; Giovanni online satellite
466 data system, NASA Goddard Earth Sciences Data and Information Services Center), reveal rather weak dust loadings
467 over the investigated region, resulting in areal N₂ fixation rates being actually inversely correlated to the satellite-
468 based average dust input ($p < 0.01$, Table S3). In contrast, satellite-based dust deposition (dry + wet) averaged over
469 the month of April 2014 (i.e. preceding the timing of sampling) indicates high fluxes over the subtropical waters
470 located south of the studied region (Fig. S3a;). The θ/S diagrams at stations Bel-11 and Bel-13 (and to a lesser extent
471 at Geo-13; Fig. S1) illustrate the presence of very warm and saline waters, which were advected from the subtropics
472 as suggested by the satellite SST images (Fig. S2). We thus argue that advection of surface waters from south of the
473 study area represented a source of atmospherically derived dFe and contributed to driving the high N₂ fixation
474 activity recorded at stations Bel-11 and Bel-13. This resulted in N₂ fixation rates there being positively (although
475 weakly) correlated ($p = 0.45$, Table S3) with the April average dust input.

476 For the central Bay of Biscay, where N₂ fixation was below the DL (stations Bel-3 and Bel-5), dust deposition in
477 April 2014 was also the lowest, suggesting that N₂ fixation there might have been limited by dFe availability. Indeed,
478 at stations Bel-3 and Bel-5 diazotrophic activity in surface waters was boosted following dFe amendments (> 25
479 nmol N L⁻¹ d⁻¹; Li et al., 2018).

480 Thus, the enhanced N₂ fixation activity at stations Bel-11 and Bel-13, as compared to the other sites, was likely
481 stimulated by the combined effects of the presence of highly competitive prymnesiophyte-UCYN-A symbionts,
482 organic matter as a source of DOP, positive P* signatures and advection of subtropical surface waters enriched in
483 dFe.

484 These statements are further supported by the outcome of a multivariate statistical analysis, providing a
485 comprehensive view of the environmental features influencing N₂ fixation. A principal component analysis (PCA;
486 Fig. 7 and Tables S2 and S5) generated two components (or axes) explaining 68% of the system's variability. Axis 1
487 illustrates the productivity of the system, or more precisely the oligotrophic state towards which it was evolving. Axis

488 1 is defined by a strong positive relation with surface temperature (reflecting the onset of stratification, particularly
489 for stations Bel-11 and Bel-13; Fig. 7) and an inverse relation with PP and associated variables (Chl *a*, NH₄⁺, NO₃⁻ +
490 NO₂⁻), which reflects the prevailing post-bloom conditions of the system. Sites characterized by a moderate (Bel-3
491 and Bel-5) to high (Bel-7, Geo-21 and to a lesser extent Geo-13) PP appear indeed tightly linked to these PP-
492 associated variables as illustrated in Fig. 7. Axis 2 is defined by the positive relation with surface salinity and P* (Fig.
493 7) and reflects the advection of surface waters of subtropical origin for stations Bel-11, Bel-13 and Geo-13. For
494 stations Geo-1 and Geo-2, the inverse relation with surface salinity (Fig. 7) is interpreted to reflect fluvial inputs
495 (Tonnard et al., 2018). Finally, this statistical analysis indicates that N₂ fixation activity was likely influenced by the
496 two PCA components, tentatively identified as productivity (axis 1) and surface water advection (axis 2) from the
497 shelf and the subtropical region.

498 5 Conclusions

499 The present work highlights the occurrence of elevated N₂ fixation activities (81–1533 μmol N m⁻² d⁻¹) in spring 2014
500 in open waters of the temperate eastern North Atlantic, off the Iberian Peninsula. These rates exceed those reported
501 by others for the Iberian Basin, but which were largely obtained outside the bloom period (from < 0.1 to 140 μmol N
502 m⁻² d⁻¹). In contrast, we did not detect any N₂ fixation activity in the central Bay of Biscay. At sites where significant
503 N₂ fixation activity was measured, rates were similar to or up to an order of magnitude larger than values reported for
504 the eastern tropical and subtropical North Atlantic, regions commonly believed to represent the main areas
505 harbouring oceanic N₂ fixation for the eastern Atlantic. Assuming that the carbon versus nitrogen requirements by
506 these N₂ fixers obeyed the Redfield stoichiometry, N₂ fixation was found to contribute 1–3% of the euphotic layer
507 daily PP and even up to 23–25% at the sites where N₂ fixation activities were the highest. The prymnesiophyte-
508 symbiont *Candidatus Atelocyanobacterium thalassa* (UCYN-A) contributed the most to the *nifH* sequences recovered
509 at the two sites where N₂ fixation activity were the highest, while the remaining sequences belonged exclusively to
510 heterotrophic bacteria. We speculate that the unexpectedly high N₂ fixation activity recorded at the time of our study
511 was sustained by (i) organic matter availability in these open waters, resulting from the prevailing vernal bloom to
512 post-bloom conditions, in combination with (ii) excess phosphorus signatures which appeared to be tightly related to
513 diazotrophic activity particularly at the two most active sites. Yet these observations and hypotheses rely on the
514 availability of dFe with evidence for input from shelf waters and pulsed atmospheric dust deposition being a
515 significant source of iron. Further studies are required to investigate this possible link between N₂ fixation activity
516 and phytoplankton bloom under iron-replete conditions in the studied region and similar environments, as these
517 would require to be considered in future assessment of global N₂ fixation.

518
519 Data availability. The data associated with the paper are available from the corresponding author upon request.
520

521 The Supplement related to this article is available.
522

523 Competing interests. The authors declare that they have no conflict of interest.
524

525 *Acknowledgements.* We thank the Captains and the crews of R/V *Belgica* and R/V *Pourquoi pas?* for their skilful
526 logistic support. A very special thank goes to the chief scientists G. Sarthou and P. Lherminier of the GEOVIDE
527 expedition for the great work experience and wonderful support on board. We would like to give special thanks to

528 Pierre Branellec, Michel Hamon, Catherine Kermabon, Philippe Le Bot, Stéphane Leizour, Olivier Ménage
529 (Laboratoire d’Océanographie Physique et Spatiale), Fabien Péroult and Emmanuel de Saint Léger (Division
530 Technique de l’INSU, Plouzané, France) for their technical expertise during clean CTD deployments. We thank A.
531 Roukaerts and D. Verstraeten for their assistance with laboratory analyses at the Vrije Universiteit Brussel. We
532 acknowledge Ryan Barkhouse for the collection of the DNA samples during the GEOVIDE cruise, Jennifer Tolman
533 and Jenni-Marie Ratten for the *nifH* amplification and Tag sequencing. P. Lherminer, P. Tréguer, E. Grossteffan, and
534 M. Le Goff are gratefully acknowledged for providing us with the shipboard physico-chemical data including CTD
535 and nitrate plus nitrite data from the GEOVIDE expedition. Shiptime for the Belgica BG2014/14 cruise was granted
536 by Operational Directorate ‘Natural Environment’ (OD Nature) of the Royal Institute of Natural Sciences, Belgium.
537 OD Nature (Ostend) is also acknowledged for their assistance in CTD operations and data acquisition on board the
538 R/V *Belgica*. This work was financed by the Flanders Research Foundation (FWO contract G0715.12N) and Vrije
539 Universiteit Brussel, R&D, Strategic Research Plan "Tracers of Past & Present Global Changes", and is a Belgian
540 contribution to SOLAS. Additional funding was provided by the Fund for Scientific Research - FNRS (F.R.S.-FNRS)
541 of the Wallonia-Brussels Federation (convention no. J.0150.15). X. Li was a FNRS doctorate Aspirant fellow
542 (mandate no. FC99216). This study was also supported, through the GEOVIDE expedition, by the French National
543 Research Agency (ANR-13-B506-0014), the Institut National des Sciences de L’Univers (INSU) of the Centre
544 National de la Recherche Scientifique (CNRS), and the French Institute for Marine Science (Ifremer). This work was
545 logistically supported for the by DT-INSU and GENAVIR. This publication is also a contribution to the Labex OT-
546 Med [ANR-11-LABEX-0061, www.otmed.fr] funded by the « Investissements d’Avenir », French Government
547 project of the French National Research Agency [ANR, www.agence-nationale-recherche.fr] through the A*Midex
548 project [ANR-11-IDEX-0001-02], funding V. Riou during the preparation of the manuscript. Finally, this work was
549 also supported by an NSERC Discovery grant and Ocean Frontier Institute (OFI) grant [Canada First Research
550 Excellence Funds] to J. LaRoche, and the OFI postdoctoral fellow D. Fonseca-Batista.

551 **References**

- 552 Agawin, N. S. R., Benavides, M., Busquets, A., Ferriol, P., Stal, L. J. and Arístegui, J.: Dominance of unicellular
553 cyanobacteria in the diazotrophic community in the Atlantic Ocean, *Limnol. Oceanogr.*, 59(2), 623–637,
554 doi:10.4319/lo.2014.59.2.0623, 2014.
- 555 Ambar, I. and Fiúza, A. F. G.: Some features of the Portugal Current System: a poleward slope undercurrent, an
556 upwelling-related summer southward flow and an autumn-winter poleward coastal surface current, in: *Proceedings of*
557 *the Second International Conference on Air-Sea Interaction and on Meteorology and Oceanography of the Coastal*
558 *Zone*, edited by: Katsaros, K. B., Fiúza, A. F. G. and Ambar, I., American Meteorological Society, Boston,
559 Massachusetts, United States, 286-287, 1994.
- 560 Benavides, M., Agawin, N., Arístegui, J., Ferriol, P. and Stal, L.: Nitrogen fixation by *Trichodesmium* and small
561 diazotrophs in the subtropical northeast Atlantic, *Aquat. Microb. Ecol.*, 65(1), 43–53, doi:10.3354/ame01534, 2011.
- 562 Blais, M., Tremblay, J.-É., Jungblut, A. D., Gagnon, J., Martin, J., Thaler, M. and Lovejoy, C.: Nitrogen fixation and
563 identification of potential diazotrophs in the Canadian Arctic, *Global Biogeochem. Cycles*, 26(3), 1–13,
564 doi:10.1029/2011GB004096, 2012.
- 565 Bombar, D., Paerl, R. W. and Riemann, L.: Marine Non-Cyanobacterial Diazotrophs: Moving beyond Molecular
566 Detection, *Trends Microbiol.*, 24(11), 916–927, doi:10.1016/j.tim.2016.07.002, 2016.

567 Bonnet, S., Dekaezemacker, J., Turk-Kubo, K. A., Moutin, T., Hamersley, R. M., Grosso, O., Zehr, J. P. and Capone,
568 D. G.: Aphotic N₂ fixation in the Eastern Tropical South Pacific Ocean., *PLoS One*, 8(12), e81265,
569 doi:10.1371/journal.pone.0081265, 2013.

570 Braun, S. T., Proctor, L. M., Zani, S., Mellon, M. T. and Zehr, J. P. Y.: Molecular evidence for zooplankton-
571 associated nitrogen-fixing anaerobes based on amplification of the nifH gene, *FEMS Microbiol. Ecol.*, 28, 273–279,
572 doi: 10.1111/j.1574-6941.1999.tb00582.x, 1999.

573 Breitbarth, E., Oschlies, A. and LaRoche, J.: Physiological constraints on the global distribution of *Trichodesmium* –
574 effect of temperature on diazotrophy, *Biogeosciences*, 4, 53–61, doi:10.5194/bg-4-53-2007, 2007.

575 Cabello, A. M., Cornejo-Castillo, F. M., Raho, N., Blasco, D., Vidal, M., Audic, S., de Vargas, C., Latasa, M.,
576 Acinas, S. G. and Massana, R.: Global distribution and vertical patterns of a prymnesiophyte–cyanobacteria obligate
577 symbiosis, *ISME J.*, 1–14, doi:10.1038/ismej.2015.147, 2015.

578 Capone, D. G.: *Trichodesmium*, a Globally Significant Marine Cyanobacterium, *Science*, 276(5316), 1221–1229,
579 doi:10.1126/science.276.5316.1221, 1997.

580 Capone, D. G., Burns, J. A., Montoya, J. P., Subramaniam, A., Mahaffey, C., Gunderson, T., Michaels, A. F. and
581 Carpenter, E. J.: Nitrogen fixation by *Trichodesmium* spp.: An important source of new nitrogen to the tropical and
582 subtropical North Atlantic Ocean, *Global Biogeochem. Cycles*, 19(2), 1–17, doi:10.1029/2004GB002331, 2005.

583 Caporaso, J. G., Kuczynski, J., Stombaugh, J., Bittinger, K., Bushman, F. D., Costello, E. K., Fierer, N., Peña, A. G.,
584 Goodrich, J. K., Gordon, J. I., Huttley, G. A., Kelley, S. T., Knights, D., Koenig, J. E., Ley, R. E., Lozupone, C. a,
585 McDonald, D., Muegge, B. D., Pirrung, M., Reeder, J., Sevinsky, J. R., Turnbaugh, P. J., Walters, W. A., Widmann,
586 J., Yatsunencko, T., Zaneveld, J. and Knight, R.: QIIME allows analysis of high- throughput community sequencing
587 data Intensity normalization improves color calling in SOLiD sequencing, *Nat. Publ. Gr.*, 7(5), 335–336,
588 doi:10.1038/nmeth0510-335, 2010.

589 Church, M. J., Jenkins, B. D., Karl, D. M. and Zehr, J. P.: Vertical distributions of nitrogen-fixing phylotypes at Stn
590 ALOHA in the oligotrophic North Pacific Ocean, *Aquat. Microb. Ecol.*, 38(1), 3–14, doi:10.3354/ame038003, 2005.

591 Comeau, A. M., Douglas, G. M. and Langille, M. G. I.: Microbiome Helper: a Custom and Streamlined Workflow for
592 Microbiome Research, *mSystems*, 2(1), e00127-16, doi:10.1128/mSystems.00127-16, 2017.

593 de Boyer Montégut, C., Madec, G., Fischer, A. S., Lazar, A., and Iudicone, D.: Mixed layer depth over the global
594 ocean: An examination of profile data and a profile-based climatology. *J. Geophys. Res.*, 109(12), 1–20,
595 doi:10.1029/2004JC002378, 2004.

596 Delmont, T. O., Quince, C., Shaiber, A., Esen, Ö. C., Lee, S. T., Rappé, M. S., McLellan, S. L., Lückner, S. and Eren,
597 A. M.: Nitrogen-fixing populations of Planctomycetes and Proteobacteria are abundant in surface ocean
598 metagenomes, *Nat. Microbiol.*, 3(8), 804–813, doi:10.1038/s41564-018-0209-4, 2018.

599 Deutsch, C., Sarmiento, J. L., Sigman, D. M., Gruber, N. and Dunne, J. P.: Spatial coupling of nitrogen inputs and
600 losses in the ocean., *Nature*, 445(7124), 163–167, doi:10.1038/nature05392, 2007.

601 Dore, J. E., Brum, J. R., Tupas, L. and Karl, D. M.: Seasonal and interannual variability in sources of nitrogen
602 supporting export in the oligotrophic subtropical North Pacific Ocean, *Limnol. Ocean.*, 47(6), 1595–1607,
603 doi:10.4319/lo.2002.47.6.1595, 2002.

604 Dyhrman, S. T. and Haley, S. T.: Phosphorus scavenging in the unicellular marine diazotroph *Crocospaera watsonii*
605 phosphorus scavenging in the unicellular marine diazotroph *Crocospaera watsonii*, *Appl. Environ. Microbiol.*, 72(2),
606 1452–1458, doi:10.1128/AEM.72.2.1452, 2006.

607 Dyhrman, S. T., Chappell, P. D., Haley, S. T., Moffett, J. W., Orchard, E. D., Waterbury, J. B. and Webb, E. A.:
608 Phosphonate utilization by the globally important marine diazotroph *Trichodesmium*, *Nature*, 439(7072), 68–71,
609 doi:10.1038/nature04203, 2006.

610 Falkowski, P. G.: Evolution of the nitrogen cycle and its influence on the biological sequestration of CO₂ in the
611 ocean, *Nature*, 387(6630), 272–275, doi:10.1038/387272a0, 1997.

612 Farnelid, H., Andersson, A. F., Bertilsson, S., Al-Soud, W. A., Hansen, L. H., Sørensen, S., Steward, G. F.,
613 Hagström, Å. and Riemann, L.: Nitrogenase gene amplicons from global marine surface waters are dominated by
614 genes of non-cyanobacteria, *PLoS One*, 6(4), doi:10.1371/journal.pone.0019223, 2011.

615 Farnelid, H., Bentzon-Tilia, M., Andersson, A. F., Bertilsson, S., Jost, G., Labrenz, M., Jürgens, K. and Riemann, L.:
616 Active nitrogen-fixing heterotrophic bacteria at and below the chemocline of the central Baltic Sea., *ISME J.*, 7(7),
617 1413–23, doi:10.1038/ismej.2013.26, 2013.

618 Fernández-Gómez, B., Richter M, Schüler M, Pinhassi, J., Acinas, S., González, J. and Pedrós-Alió, C.: Ecology of
619 marine Bacteroidetes: a comparative genomics approach, *ISME J.*, 7(5), 1026–1037, doi:10.1038/ismej.2012.169,
620 2013.

621 Fernández, A., Mouriño-Carballido, B., Bode, A., Varela, M. and Marañón, E.: Latitudinal distribution of
622 *Trichodesmium* spp. and N₂ fixation in the Atlantic Ocean, *Biogeosciences*, 7(2), 3167–3176, doi:10.5194/bg-7-
623 3167-2010, 2010.

624 Fernández I., C., Raimbault, P., Garcia, N. and Rimmelin, P.: An estimation of annual new production and carbon
625 fluxes in the northeast Atlantic Ocean during 2001, *J. Geophys. Res.*, 110(C7), 1–15, doi:10.1029/2004JC002616,
626 2005.

627 Fiúza, A.F.G.: Hidrologia e dinâmica das águas costeiras de Portugal (Hydrology and dynamics of the Portuguese
628 coastal waters), Ph.D. thesis, Universidade de Lisboa, Portugal, 294 pp., 1984.

629 Fonseca-Batista, D., Dehairs, F., Riou, V., Fripiat, F., Elskens, M., Deman, F., Brion, N., Quéroué, F., Bode, M. and
630 Auel, H.: Nitrogen fixation in the eastern Atlantic reaches similar levels in the Southern and Northern Hemisphere, *J.*
631 *Geophys. Res. Ocean.*, 122, 4618–4632, doi:10.1002/2016JC012335, 2017.

632 Foster, R. A., Subramaniam, A., Mahaffey, C., Carpenter, E. J., Capone, D. G. and Zehr, J. P.: Influence of the
633 Amazon River plume on distributions of free-living and symbiotic cyanobacteria in the western tropical north
634 Atlantic Ocean, *Limnol. Oceanogr.*, 52(2), 517–532, doi:10.4319/lo.2007.52.2.0517, 2007.

635 Frouin, R., Fiúza, A. F. G., Ambar, I. and Boyd, T. J.: Observations of a poleward surface current off the coasts of
636 Portugal and Spain during winter, *J. Geophys. Res.*, 95(C1), 679, doi:10.1029/JC095iC01p00679, 1990.

637 García-Ibáñez, M. I., Pardo, P. C., Carracedo, L. I., Mercier, H., Lherminier, P., Ríos, A. F. and Pérez, F. F.:
638 Structure, transports and transformations of the water masses in the Atlantic Subpolar Gyre, *Prog. Oceanogr.*, 135,
639 18–36, doi:10.1016/j.pocean.2015.03.009, 2015.

640 Garcia, H. E., Locarnini, R. A., Boyer, T. P., Antonov, J. I., Baranova, O. K., Zweng, M. M., Reagan, J. R. and
641 Johnson, D. R.: *World Ocean Atlas 2013, Volume 4: Dissolved Inorganic Nutrients (phosphate, nitrate, silicate)*,
642 edited by: S. Levitus and A. Mishonov, National Oceanographic Data Center, Silver Spring, Maryland, USA., 2013.

643 Grasshoff, K., Ehrhardt, M. and Kremling, K. (Eds.): *Methods of Seawater Analysis. Second, Revised and Extended*
644 *Edition*, Verlag Chemie GmbH, Weinheim, Germany, 1983.

645 Großkopf, T., Mohr, W., Baustian, T., Schunck, H., Gill, D., Kuypers, M. M. M., Lavik, G., Schmitz, R. A., Wallace,
646 D. W. R. and LaRoche, J.: Doubling of marine dinitrogen-fixation rates based on direct measurements, *Nature*,
647 488(7411), 361–364, doi:10.1038/nature11338, 2012.

648 Gruber, N.: The Marine Nitrogen Cycle: Overview and Challenges, in: Nitrogen in the Marine Environment, edited
649 by: Capone, D. G., Bronk, D. A., Mulholland, M. M., Carpenter E. J., Academic Press, Cambridge, Massachusetts,
650 United States, 1–50, <https://doi.org/10.1016/B978-0-12-372522-6.X0001-1>, 2008.

651 Halm, H., Lam, P., Ferdelman, T. G., Lavik, G., Dittmar, T., LaRoche, J., D’Hondt, S. and Kuypers, M. M. M.:
652 Heterotrophic organisms dominate nitrogen fixation in the South Pacific Gyre., *ISME J.*, 6(6), 1238–49,
653 doi:10.1038/ismej.2011.182, 2012.

654 Hama, T., Miyazaki, T., Ogawa, Y., Iwakuma, T., Takahashi, M., Otsuki, A. and Ichimura, S.: Measurement of
655 photosynthetic production of a marine phytoplankton population using a stable ¹³C isotope, *Mar. Biol.*, 73, 31–36,
656 doi:10.1007/BF00396282, 1983.

657 Holmes, R. M., Aminot, A., K  rouel, R., Hooker, B. A. and Peterson, B. J.: A simple and precise method for
658 measuring ammonium in marine and freshwater ecosystems, *Can. J. Fish. Aquat. Sci.*, 56(10), 1801–1808,
659 doi:10.1139/f99-128, 1999.

660 Howard, J. B. and Rees, D. C.: Structural Basis of Biological Nitrogen Fixation., *Chem. Rev.*, 96(7), 2965–2982,
661 doi:10.1021/cr9500545, 1996.

662 Inoue, J., Oshima, K., Suda, W., Sakamoto, M., Iino, T., Noda, S., Hongoh, Y., Hattori, M. and Ohkuma, M.:
663 Distribution and evolution of nitrogen fixation genes in the phylum Bacteroidetes., *Microbes Environ.*, 30(1), 44–50,
664 doi:10.1264/jsme2.ME14142, 2015.

665 Jickells, T. D.: The inputs of dust derived elements to the Sargasso Sea; a synthesis, *Mar. Chem.*, 68(1–2), 5–14,
666 doi:10.1016/S0304-4203(99)00061-4, 1999.

667 Khadem, A. F., Pol, A., Jetten, M. S. M. and Op Den Camp, H. J. M.: Nitrogen fixation by the verrucomicrobial
668 methanotroph “*Methylacidiphilum fumariolicum*” SolV, *Microbiology*, 156(4), 1052–1059,
669 doi:10.1099/mic.0.036061-0, 2010.

670 Kimura, M.: A simple method for estimating evolutionary rates of base substitutions through comparative studies of
671 nucleotide sequences, *J. Mol. Evol.*, 16(2), 111–120, doi:10.1007/BF01731581, 1980.

672 Krupke, A., Lavik, G., Halm, H., Fuchs, B. M., Amann, R. I. and Kuypers, M. M. M.: Distribution of a consortium
673 between unicellular algae and the N₂ fixing cyanobacterium UCYN-A in the North Atlantic Ocean, *Environ.*
674 *Microbiol.*, 16(10), 3153–3167, doi:10.1111/1462-2920.12431, 2014.

675 Kumar, S., Stecher, G. and Tamura, K.: MEGA7: Molecular Evolutionary Genetics Analysis version 7.0 for bigger
676 datasets., *Mol. Biol. Evol.*, msw054, doi:10.1093/molbev/msw054, 2016.

677 Landolfi, A., Koeve, W., Dietze, H., K  hler, P. and Oschlies, A.: A new perspective on environmental controls,
678 *Geophys. Res. Lett.*, 42(May), 4482–2289, doi.org/10.1002/2015GL063756, 2015.

679 Langlois, R., Gro  kopf, T., Mills, M., Takeda, S. and LaRoche, J.: Widespread Distribution and Expression of
680 Gamma A (UMB), an Uncultured, Diazotrophic, γ -Proteobacterial nifH Phylotype., *PLoS One*, 10(6), e0128912,
681 doi:10.1371/journal.pone.0128912, 2015.

682 Langlois, R. J., LaRoche, J. and Raab, P. A.: Diazotrophic Diversity and Distribution in the Tropical and Subtropical
683 Atlantic Ocean Diazotrophic Diversity and Distribution in the Tropical and Subtropical Atlantic Ocean, *Appl.*
684 *Environ. Microbiol.*, 71(12), 7910–7919, doi:10.1128/AEM.71.12.7910, 2005.

685 Langlois, R. J., H  mmer, D. and LaRoche, J.: Abundances and distributions of the dominant nifH phylotypes in the
686 Northern Atlantic Ocean, *Appl. Environ. Microbiol.*, 74(6), 1922–1931, doi:10.1128/AEM.01720-07, 2008.

687 Lemaitre, N., Planchon, F., Planquette, H., Dehairs, F., Fonseca-Batista, D., Roukaerts, A., Deman, F., Tang, Y.,
688 Mariez, C. and Sarthou, G.: High variability of export fluxes along the North Atlantic GEOTRACES section GA01:

689 Particulate organic carbon export deduced from the ^{234}Th method, *Biogeosciences Discuss.*, (April), 1–38,
690 doi:10.5194/bg-2018-190, 2018.

691 Li, X., Fonseca-Batista, D., Roevros, N., Dehairs, F. and Chou, L.: Environmental and nutrient controls of marine
692 nitrogen fixation, *Prog. Oceanogr.*, 167(August), 125–137, doi:10.1016/j.pocean.2018.08.001, 2018.

693 Loescher, C. R., Großkopf, T., Desai, F. D., Gill, D., Schunck, H., Croot, P. L., Schlosser, C., Neulinger, S. C.,
694 Pinnow, N., Lavik, G., Kuypers, M. M. M., Laroche, J. and Schmitz, R. A.: Facets of diazotrophy in the oxygen
695 minimum zone waters off Peru, *ISME J.*, 8(11), 2180–2192, doi:10.1038/ismej.2014.71, 2014.

696 Luo, H., Benner, R., Long, R. a and Hu, J.: Subcellular localization of marine bacterial alkaline phosphatases., *Proc.*
697 *Natl. Acad. Sci. U. S. A.*, 106(50), 21219–21223, doi:10.1073/pnas.0907586106, 2009.

698 Luo, Y.-W., Doney, S. C., Anderson, L. A., Benavides, M., Berman-Frank, I., Bode, A., Bonnet, S., Boström, K. H.,
699 Böttjer, D., Capone, D. G., Carpenter, E. J., Chen, Y. L., Church, M. J., Dore, J. E., Falcón, L. I., Fernández, A.,
700 Foster, R. A., Furuya, K., Gómez, F., Gundersen, K., Hynes, A. M., Karl, D. M., Kitajima, S., Langlois, R. J.,
701 LaRoche, J., Letelier, R. M., Marañón, E., McGillicuddy, D. J., Moisaner, P. H., Moore, C. M., Mouriño-Carballido,
702 B., Mulholland, M. R., Needoba, J. A., Orcutt, K. M., Poulton, A. J., Rahav, E., Raimbault, P., Rees, A. P., Riemann,
703 L., Shiozaki, T., Subramaniam, A., Tyrrell, T., Turk-Kubo, K. A., Varela, M., Villareal, T. A., Webb, E. A., White,
704 A. E., Wu, J. and Zehr, J. P.: Database of diazotrophs in global ocean: abundance, biomass and nitrogen fixation
705 rates, *Earth Syst. Sci. Data*, 4(1), 47–73, doi:10.5194/essd-4-47-2012, 2012.

706 Luo, Y.-W., Lima, I. D., Karl, D. M., Deutsch, C. A. and Doney, S. C.: Data-based assessment of environmental
707 controls on global marine nitrogen fixation, *Biogeosciences*, 11(3), 691–708, doi:10.5194/bg-11-691-2014, 2014.

708 Man-Aharonovich, D., Kress, N., Zeev, E. B., Berman-Frank, I. and Béjà, O.: Molecular ecology of *nifH* genes and
709 transcripts in the eastern Mediterranean Sea, *Environ. Microbiol.*, 9(9), 2354–2363, doi:10.1111/j.1462-
710 2920.2007.01353.x, 2007.

711 Marañón, E., Holligan, P. M., Varela, M., Mouriño, B. and Bale, A. J.: Basin-scale variability of phytoplankton
712 biomass, production and growth in the Atlantic Ocean, *Deep Sea Res. Part I Oceanogr. Res. Pap.*, 47(5), 825–857,
713 doi:10.1016/S0967-0637(99)00087-4, 2000.

714 Martínez-Pérez, C., Mohr, W., Löscher, C. R., Dekaezemacker, J., Littmann, S., Yilmaz, P., Lehnen, N., Fuchs, B.
715 M., Lavik, G., Schmitz, R. A., LaRoche, J. and Kuypers, M. M. M.: The small unicellular diazotrophic symbiont,
716 UCYN-A, is a key player in the marine nitrogen cycle, *Nat. Microbiol.*, 1(September), 1–7,
717 doi:10.1038/nmicrobiol.2016.163, 2016.

718 McCartney, M. S. and Talley, L. D.: The Subpolar Mode Water of the North Atlantic Ocean, *J. Phys. Oceanogr.*,
719 12(11), 1169–1188, doi:10.1175/1520-0485(1982)012<1169:TSMWOT>2.0.CO;2, 1982.

720 Mills, M. M., Ridame, C., Davey, M., La Roche, J. and Geider, R. J.: Iron and phosphorus co-limit nitrogen fixation
721 in the eastern tropical North Atlantic, *Nature*, 429(May), 292–294, doi:10.1038/nature02550, 2004.

722 Miyajima, T., Yamada, Y., Hanaba, Y. T., Yoshii, K., Koitabashi, K. and Wada, E.: Determining the stable isotope
723 ratio of total dissolved inorganic carbon in lake water by GC/C/IRMS, *Limnol. Oceanogr.*, 40(5), 994–1000,
724 doi:10.4319/lo.1995.40.5.0994, 1995.

725 Mohr, W., Großkopf, T., Wallace, D. W. R. and LaRoche, J.: Methodological underestimation of oceanic nitrogen
726 fixation rates, *PLoS One*, 5(9), 1–7, doi:10.1371/journal.pone.0012583, 2010.

727 Montoya, J. P., Voss, M., Kahler, P. and Capone, D. G.: A Simple, High-Precision, High-Sensitivity Tracer Assay for
728 N_2 Fixation, *Appl. Environ. Microbiol.*, 62(3), 986–993, 1996.

729 Montoya, J. P., Voss, M. and Capone, D. G.: Spatial variation in N_2 -fixation rate and diazotroph activity in the
730 Tropical Atlantic, *Biogeosciences*, 4(3), 369–376, doi:10.5194/bg-4-369-2007, 2007.

731 Moore, C. M., Mills, M. M., Achterberg, E. P., Geider, R. J., LaRoche, J., Lucas, M. I., McDonagh, E. L., Pan, X.,
732 Poulton, A. J., Rijkenberg, M. J. A., Suggett, D. J., Ussher, S. J. and Woodward, E. M. S.: Large-scale distribution of
733 Atlantic nitrogen fixation controlled by iron availability, *Nat. Geosci.*, 2(12), 867–871, doi:10.1038/ngeo667, 2009.

734 Moreira-Coello, V., Mouriño-Carballido, B., Marañón, E., Fernández-Carrera, A., Bode, A. and Varela, M. M.:
735 Biological N₂ Fixation in the Upwelling Region off NW Iberia: Magnitude, Relevance, and Players, *Front. Mar. Sci.*,
736 4(September), doi:10.3389/fmars.2017.00303, 2017.

737 Mulholland, M. R., Bernhardt, P. W., Blanco-Garcia, J. L., Mannino, A., Hyde, K., Mondragon, E., Turk, K.,
738 Moisander, P. H. and Zehr, J. P.: Rates of dinitrogen fixation and the abundance of diazotrophs in North American
739 coastal waters between Cape Hatteras and Georges Bank, *Limnol. Oceanogr.*, 57(4), 1067–1083,
740 doi:10.4319/lo.2012.57.4.1067, 2012.

741 Needoba, J. A., Foster, R. A., Sakamoto, C., Zehr, J. P. and Johnson, K. S.: Nitrogen fixation by unicellular
742 diazotrophic cyanobacteria in the temperate oligotrophic North Pacific Ocean, *Limnol. Oceanogr.*, 52(4), 1317–1327,
743 doi:10.4319/lo.2007.52.4.1317, 2007.

744 Nei, M. (Eds.): *Molecular Evolutionary Genetics*, Columbia University Press, New York, United States, 1987.

745 Ohlendieck, U., Stuhr, A. and Siegmund, H.: Nitrogen fixation by diazotrophic cyanobacteria in the Baltic Sea and
746 transfer of the newly fixed nitrogen to picoplankton organisms, *J. Mar. Syst.*, 25(3–4), 213–219, doi:10.1016/S0924-
747 7963(00)00016-6, 2000.

748 Poulton, A. J., Holligan, P. M., Hickman, A., Kim, Y. N., Adey, T. R., Stinchcombe, M. C., Holeton, C., Root, S. and
749 Woodward, E. M. S.: Phytoplankton carbon fixation, chlorophyll-biomass and diagnostic pigments in the Atlantic
750 Ocean, *Deep. Res. Part II Top. Stud. Oceanogr.*, 53(14–16), 1593–1610, doi:10.1016/j.dsr2.2006.05.007, 2006.

751 Rahav, E., Bar-Zeev, E., Ohayon, S., Elifantz, H., Belkin, N., Herut, B., Mulholland, M. R. and Berman-Frank, I.:
752 Dinitrogen fixation in aphotic oxygenated marine environments, *Front. Microbiol.*, 4(AUG), 1–11,
753 doi:10.3389/fmicb.2013.00227, 2013.

754 Rahav, E., Giannetto, M. J. and Bar-Zeev, E.: Contribution of mono and polysaccharides to heterotrophic N₂ fixation
755 at the eastern Mediterranean coastline, *Sci. Rep.*, 6(May), 1–11, doi:10.1038/srep27858, 2016.

756 Ras, J., Claustre, H. and Uitz, J.: Spatial variability of phytoplankton pigment distributions in the Subtropical South
757 Pacific Ocean: comparison between in situ and predicted data, *Biogeosciences*, 5, 353–369, doi:10.5194/bgd-4-3409-
758 2007, 2008.

759 Ratten, J.-M.: The diversity, distribution and potential metabolism of non-cyanobacterial diazotrophs in the North
760 Atlantic Ocean, Ph.D. thesis, Dalhousie University, Nova Scotia, Canada, 485 pp., 2017.

761 Ratten, J. M., LaRoche, J., Desai, D. K., Shelley, R. U., Landing, W. M., Boyle, E., Cutter, G. A. and Langlois, R. J.:
762 Sources of iron and phosphate affect the distribution of diazotrophs in the North Atlantic, *Deep. Res. Part II Top.*
763 *Stud. Oceanogr.*, 116, 332–341, doi:10.1016/j.dsr2.2014.11.012, 2015.

764 Raven, J. A.: The iron and molybdenum use efficiencies of plant growth with different energy, carbon and nitrogen
765 sources, *New Phytol.*, 109, 279–287, doi:10.1111/j.1469-8137.1988.tb04196.x, 1988.

766 Rees, A., Gilbert, J. and Kelly-Gerreyn, B.: Nitrogen fixation in the western English Channel (NE Atlantic Ocean),
767 *Mar. Ecol. Prog. Ser.*, 374(1979), 7–12, doi:10.3354/meps07771, 2009.

768 Rijkenberg, M. J. A., Langlois, R. J., Mills, M. M., Patey, M. D., Hill, P. G., Nielsdóttir, M. C., Compton, T. J.,
769 LaRoche, J. and Achterberg, E. P.: Environmental forcing of nitrogen fixation in the Eastern Tropical and Sub-
770 Tropical North Atlantic Ocean, *PLoS One*, 6(12), doi:10.1371/journal.pone.0028989, 2011.

771 Riou, V., Fonseca-Batista, D., Roukaerts, A., Biegala, I. C., Prakya, S. R., Magalhães Loureiro, C., Santos, M.,
772 Muniz-Piniella, A. E., Schmiing, M., Elskens, M., Brion, N., Martins, M. A. and Dehairs, F.: Importance of N₂-

773 Fixation on the Productivity at the North-Western Azores Current/Front System, and the Abundance of Diazotrophic
774 Unicellular Cyanobacteria, *PLoS One*, 11(3), e0150827, doi:10.1371/journal.pone.0150827, 2016.

775 Sarthou, G., Baker, A. R., Blain, S., Achterberg, E. P., Boye, M., Bowie, A. R., Croot, P., Laan, P., De Baar, H. J.
776 W., Jickells, T. D. and Worsfold, P. J.: Atmospheric iron deposition and sea-surface dissolved iron concentrations in
777 the eastern Atlantic Ocean, *Deep. Res. Part I Oceanogr. Res. Pap.*, 50(10–11), 1339–1352, doi:10.1016/S0967-
778 0637(03)00126-2, 2003.

779 Scavotto, R. E., Dziallas, C., Bentzon-Tilia, M., Riemann, L. and Moisander, P. H.: Nitrogen-fixing bacteria
780 associated with copepods in coastal waters of the North Atlantic Ocean, *Environ. Microbiol.*, 17(10), 3754–3765,
781 doi:10.1111/1462-2920.12777, 2015.

782 Shelley, R. U., Roca-Martí, M., Castrillejo, M., Sanial, V., Masqué, P., Landing, W. M., van Beek, P., Planquette, H.
783 and Sarthou, G.: Quantification of trace element atmospheric deposition fluxes to the Atlantic Ocean (> 40°N;
784 GEOVIDE, GEOTRACES GA01) during spring 2014, *Deep. Res. Part I*, 119(November 2016), 34–49,
785 doi:10.1016/j.dsr.2016.11.010, 2017.

786 Shiozaki, T., Ijichi, M., Kodama, T., Takeda, S., Furuya, K., Ijichi, M., Kodama, T., Takeda, S. and Furuya, K.:
787 Heterotrophic bacteria as major nitrogen fixers in the euphotic zone of the Indian Ocean, *Global Biogeochem.*
788 *Cycles*, 28, 1096–1110, doi.org/10.1002/2014GB004886, 2014.

789 Shiozaki, T., Nagata, T., Ijichi, M. and Furuya, K.: Nitrogen fixation and the diazotroph community in the temperate
790 coastal region of the northwestern North Pacific, *Biogeosciences*, 12(15), 4751–4764, doi:10.5194/bg-12-4751-2015,
791 2015.

792 Snow, J. T., Schlosser, C., Woodward, E. M. S., Mills, M. M., Achterberg, E. P., Mahaffey, C., Bibby, T. S. and
793 Moore, C. M.: Environmental controls on the biogeography of diazotrophy and *Trichodesmium* in the Atlantic
794 Ocean, *Global Biogeochem. Cycles*, 29, 865–884, doi.org/10.1002/2015GB005090, 2015.

795 Subramaniam, A., Yager, P. L., Carpenter, E. J., Mahaffey, C., Björkman, K., Cooley, S., Kustka, A. B., Montoya, J.
796 P., Sañudo-Wilhelmy, S. A., Shipe, R. and Capone, D. G.: Amazon River enhances diazotrophy and carbon
797 sequestration in the tropical North Atlantic Ocean, *Global Biogeochem. Cycles*, 105, 10460–10465,
798 doi:10.1029/2006GB002751, 2008.

799 Subramaniam, A., Mahaffey, C., Johns, W. and Mahowald, N.: Equatorial upwelling enhances nitrogen fixation in
800 the Atlantic Ocean, *Geophys. Res. Lett.*, 40(9), 1766–1771, doi:10.1002/grl.50250, 2013.

801 Thompson, A. W., Foster, R. A., Krupke, A., Carter, B. J., Musat, N., Vaulot, D., Kuypers, M. M. M. and Zehr, J. P.:
802 Unicellular Cyanobacterium Symbiotic with a Single-Celled Eukaryotic Alga, *Science*, 337(September), 1546–1550,
803 doi:10.1126/science.1222700, 2012.

804 Thuróczy, C.-E., Gerringa, L. J. A., Klunder, M. B., Middag, R., Laan, P., Timmermans, K. R. and de Baar, H. J. W.:
805 Speciation of Fe in the Eastern North Atlantic Ocean, *Deep Sea Res. Part I Oceanogr. Res. Pap.*, 57(11), 1444–1453,
806 doi:10.1016/j.dsr.2010.08.004, 2010.

807 Tonnard, M., Planquette, H., Bowie, A. R., van der Merwe, P., Gallinari, M., Deprez de Gesincourt, F., Germain, Y.,
808 Gourain, A., Benetti, M., Reverdin, G., Treguer, P., Boutorh, J., Cheize, M., Menzel Barraqueta, J.-L., Pereira-
809 Contraira, L., Shelley, R., Lherminier, P. and Sarthou, G.: Dissolved iron distribution in the North Atlantic Ocean and
810 Labrador Sea along the GEOVIDE section (GEOTRACES section GA01), *Biogeosciences Discuss.*, (April), 2018.

811 Vidal, M., Duarte, C. M. and Agustí, S.: Dissolved organic nitrogen and phosphorus pools and fluxes in the central
812 Atlantic Ocean, *Limnol. Oceanogr.*, 44(1), 106–115, doi:10.4319/lo.1999.44.1.0106, 1999.

813 Vidal, M., Duarte, C. M., Agustí, S., Gasol, J. M. and Vaqué, D.: Alkaline phosphatase activities in the central
814 Atlantic Ocean indicate large areas with phosphorus deficiency, *Mar. Ecol. Prog. Ser.*, 262, 43–53,
815 doi:10.3354/meps262043, 2003.

816 Villa-Alfageme, M., de Soto, F. C., Ceballos, E., Giering, S. L. C., Le Moigne, F. A. C., Henson, S., Mas, J. L. and
817 Sanders, R. J.: Geographical, seasonal, and depth variation in sinking particle speeds in the North Atlantic, *Geophys.*
818 *Res. Lett.*, 43, 8609–8616, doi:10.1002/2016GL069233, 2016.

819 Voss, M., Croot, P., Lochte, K., Mills, M. and Peeken, I.: Patterns of nitrogen fixation along 10°N in the tropical
820 Atlantic, *Geophys. Res. Lett.*, 31(23), 1–4, doi:10.1029/2004GL020127, 2004.

821 Wertz, J. T., Kim, E., Breznak, J. A., Schmidt, T. M. and Rodrigues, J. L. M.: Genomic and physiological
822 characterization of the Verrucomicrobia isolate *Diplosphaera colitermitum* gen. nov., sp. nov., reveals microaerophily
823 and nitrogen fixation genes, *Appl. Environ. Microbiol.*, 78(5), 1544–1555, doi:10.1128/AEM.06466-11, 2012.

824 Yentsch, C. S. and Menzel, D. W.: A method for the determination of phytoplankton chlorophyll and phaeophytin by
825 fluorescence, *Deep Sea Res. Oceanogr. Abstr.*, 10(3), 221–231, doi:10.1016/0011-7471(63)90358-9, 1963.

826 Zani, S., Mellon, M. T., Collier, J. L. and Zehr, J. P.: Expression of *nifH* genes in natural microbial assemblages in
827 Lake George, New York, detected by reverse transcriptase PCR, *Appl. Environ. Microbiol.*, 66(7), 3119–3124,
828 doi:10.1128/AEM.66.7.3119-3124.2000, 2000.

829 Zeebe, R. E. and Wolf-Gladrow, D.: *CO₂ in seawater: equilibrium, kinetics, isotopes*, Elsevier Science, Amsterdam,
830 The Netherlands, 2003.

831 **Table**

832

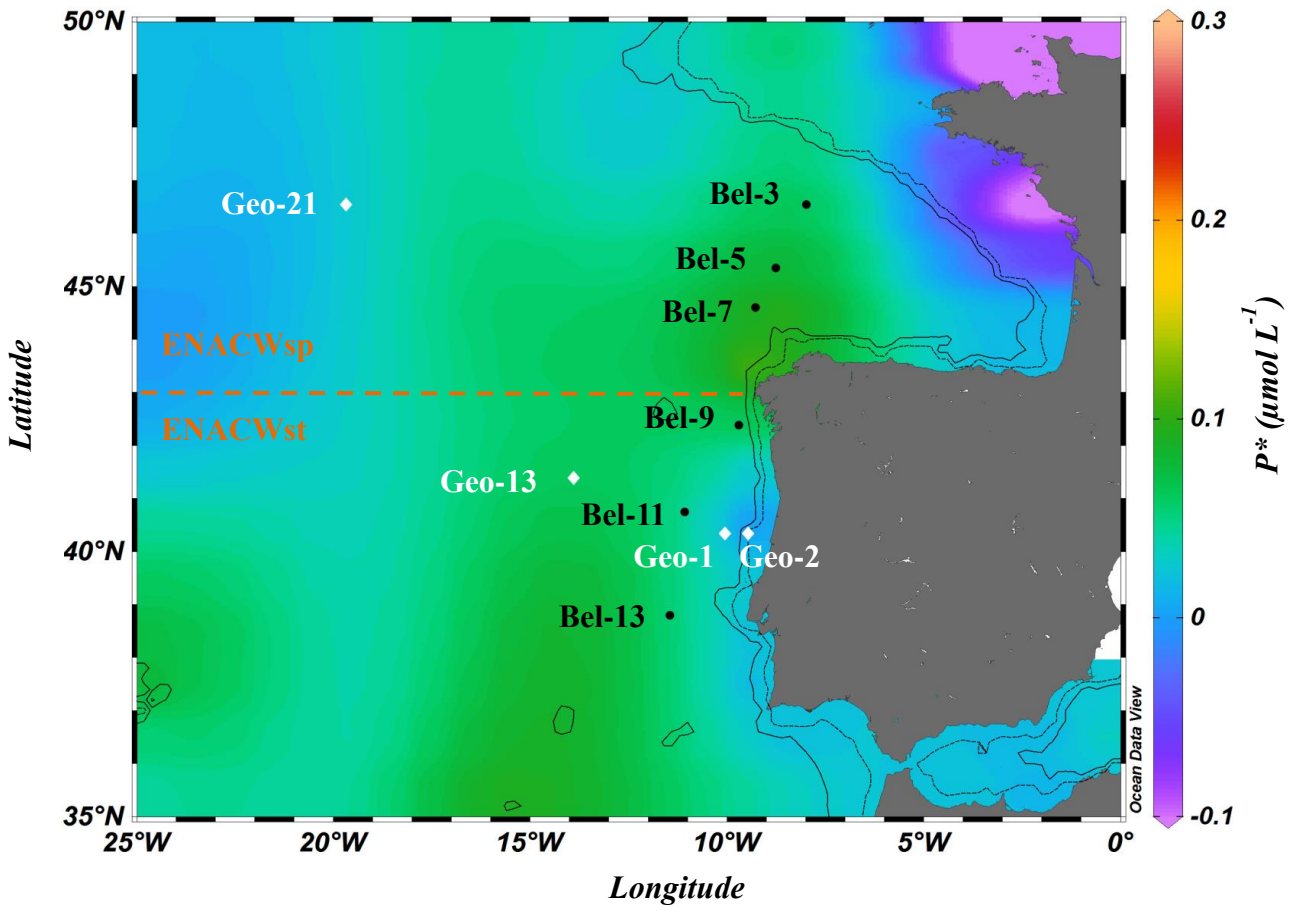
833

834 **Table 1:** Relative contribution (%) of N₂ fixation to Primary Production (PP).

835

Province	Station	Latitude (° N)	Longitude (° E)	N ₂ fixation contribution to PP (%) (Redfield 6.6 ratio)	SD	N ₂ fixation contribution to PP (%) (mean POC/PN ratio of 6.3 ± 1.1)	SD
ENACW _{sp}	Bel-3	46.5	-8.0	0	-	0	-
	Bel-5	45.3	-8.8	0	-	0	-
	Bel-7	44.6	-9.3	2	0.4	1	0.4
	Geo-21	46.5	-19.7	1	0.02	1	0.0
ENACW _{st}	Bel-9	42.4	-9.7	1	0.1	1	0.1
	Bel-11	40.7	-11.1	28	1.9	25	1.8
	Bel-13	38.8	-11.4	25	1.3	23	1.2
	Geo-1	40.3	-10.0	3	0.2	3	0.1
	Geo-2	40.3	-9.5	3	0.1	3	0.1
	Geo-13	41.4	-13.9	3	0.1	3	0.1

836

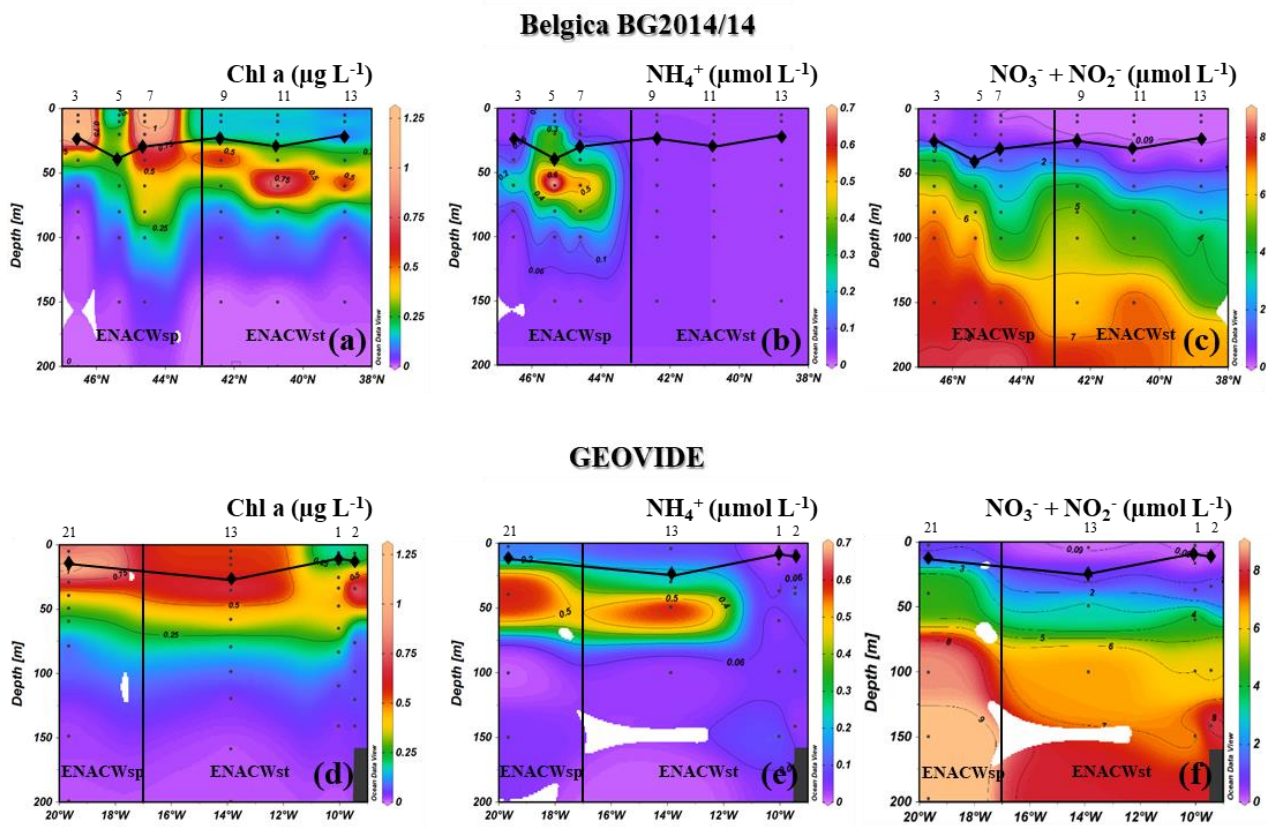


840

841 **Figure 1:** Location of sampling stations during the Belgica BG2014/14 (black labels) and GEOVIDE (white labels)
 842 cruises (May 2014) superimposed on a map of the seasonal average phosphate excess ($P^* = [\text{PO}_4^{3-}] - [\text{NO}_3^-] / 16$) at
 843 20 m (April to June for the period from 1955 to 2012; World Ocean Atlas 2013; Garcia et al., 2013). Areas of
 844 dominance of the Eastern North Atlantic Central Waters of subpolar (ENACWsp) and subtropical (ENACWst) origin
 845 are separated by a horizontal dashed line. Black dashed and solid contour lines illustrate 500 m and 1500 m isobaths,
 846 respectively. (Schlitzer, R., Ocean Data View).

847

848



849

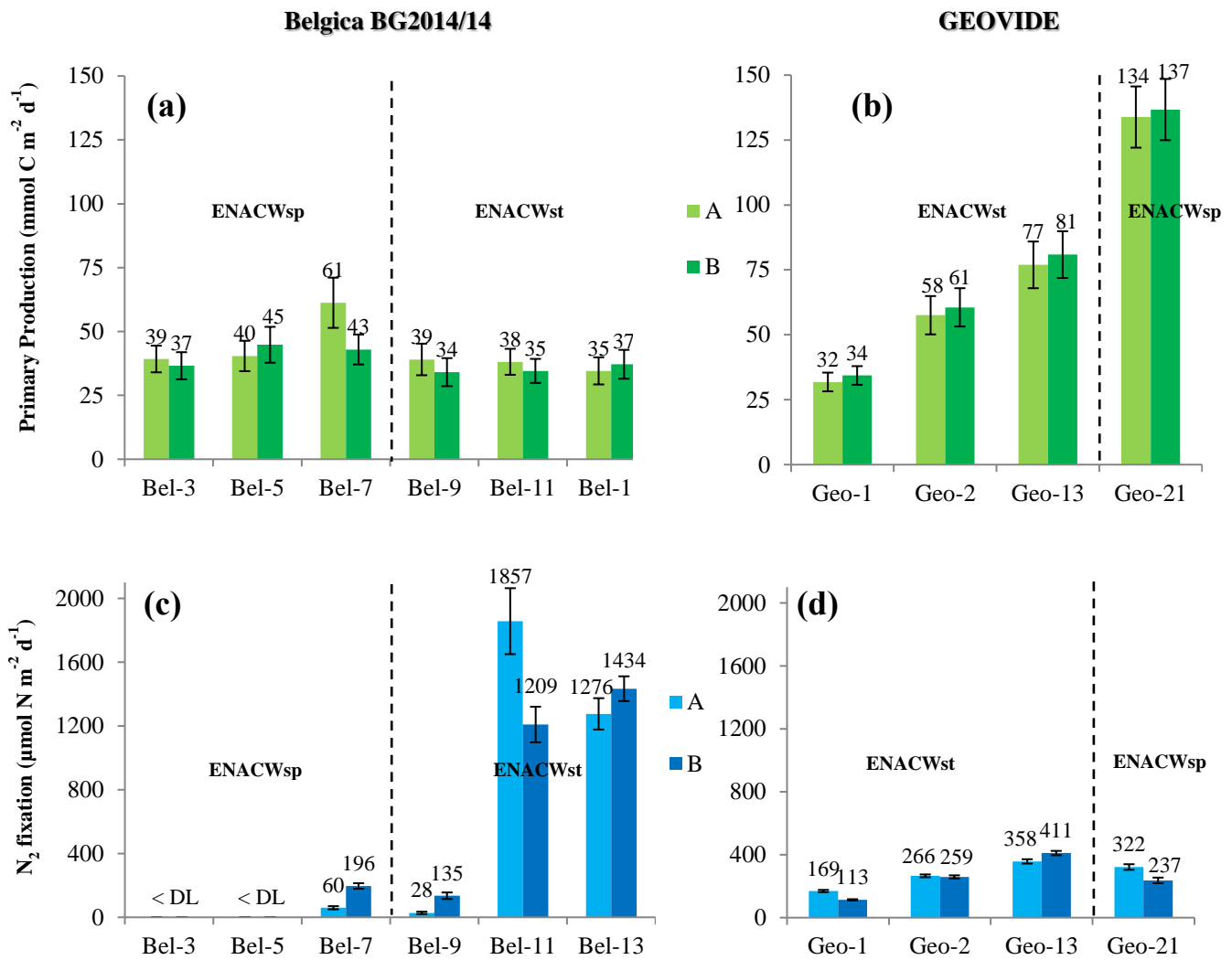
850

851

852 **Figure 2:** Spatial distribution of Chl *a* (a, d), NH₄⁺ (b, e) and NO₃⁻ + NO₂⁻ (c, f) concentrations along the Belgica
853 BG2014/14 (upper panels) and GEOVIDE (lower panels) cruise tracks. Station numbers are indicated above the
854 sections. The vertical black line represents the boundary between areas with dominance of Eastern North Atlantic
855 Waters of subpolar (ENACWsp) and subtropical (ENACWst) origin. Mixed layer depth (MLD, black lines
856 connecting diamonds) was estimated using a temperature threshold criterion of 0.2 °C relative to the temperature at
857 10 m (de Boyer Montégut et al., 2004). (Schlitzer, R., Ocean Data View).

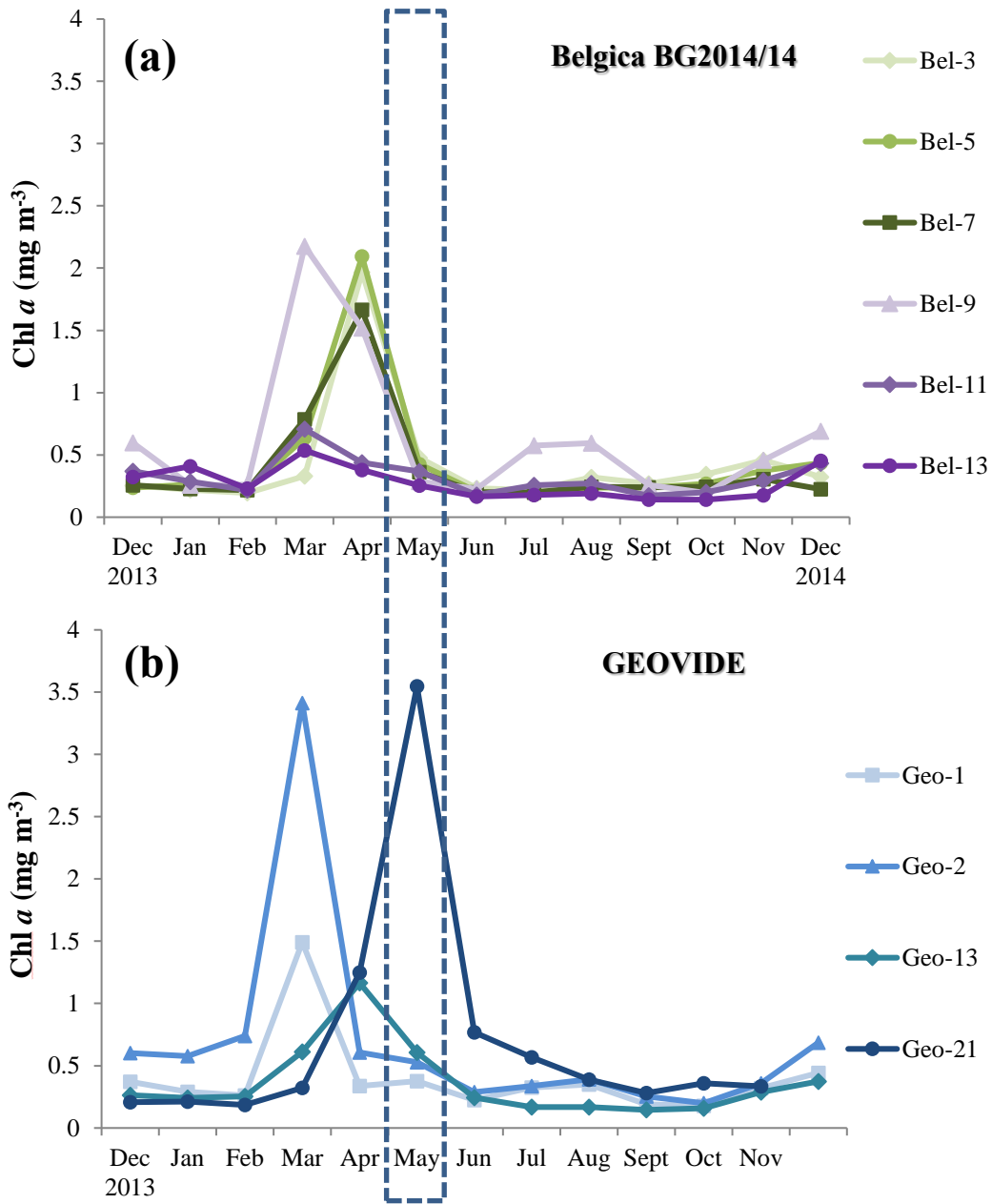
858

859



860

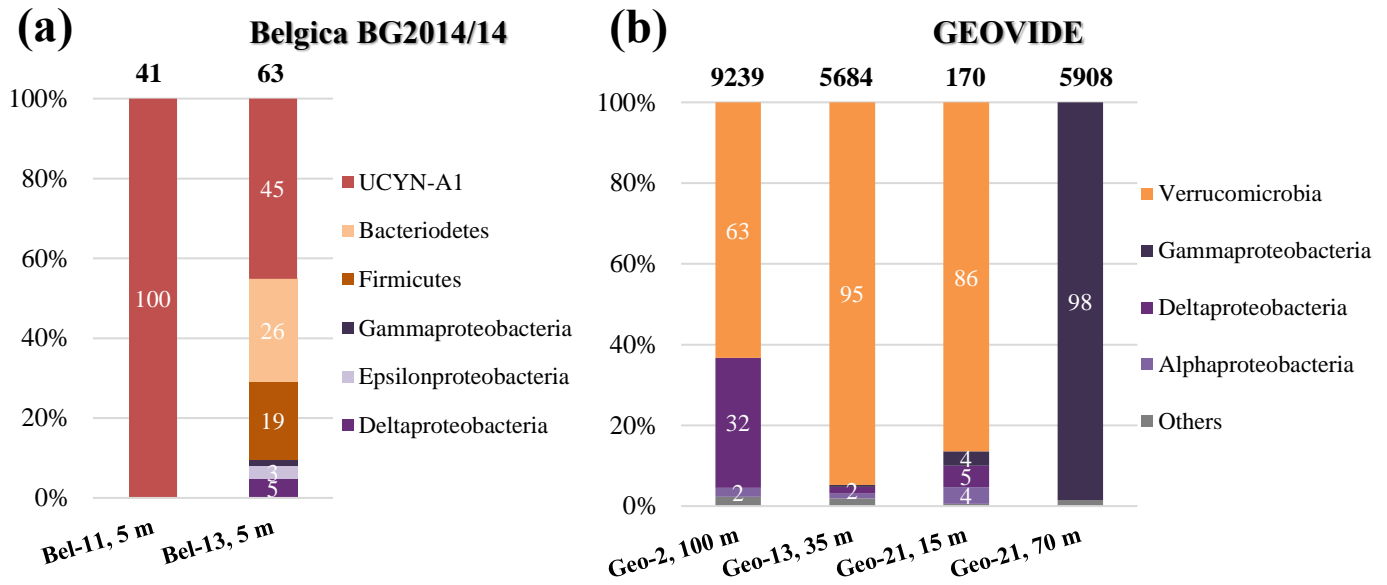
861 **Figure 3:** Spatial distribution (\pm SD) of depth-integrated rates of primary production (**a, b**) (duplicates are in light
 862 and dark green bars with the corresponding values in mmol C m⁻² d⁻¹); N₂ fixation (**c, d**) (duplicates are in light and
 863 dark blue bars with the corresponding values in μ mol N m⁻² d⁻¹) determined during the Belgica BG2014/14 (**a, c**) and
 864 GEOVIDE (**b, d**) cruises. Error bars represent the propagated measurement uncertainty of all parameters used to
 865 compute volumetric uptake rates.



869 **Figure 4:** Time series of area-averaged chlorophyll a concentration (mg m^{-3}) registered by Aqua MODIS satellite
 870 (Giovanni online satellite data system) between December 2013 and December 2014 for the $0.5^\circ \times 0.5^\circ$ grid
 871 surrounding the different stations during the **(a)** Belgica BG2014/14 and **(b)** GEOVIDE cruises. The dashed box
 872 highlights the sampling period for both cruises (May 2014).

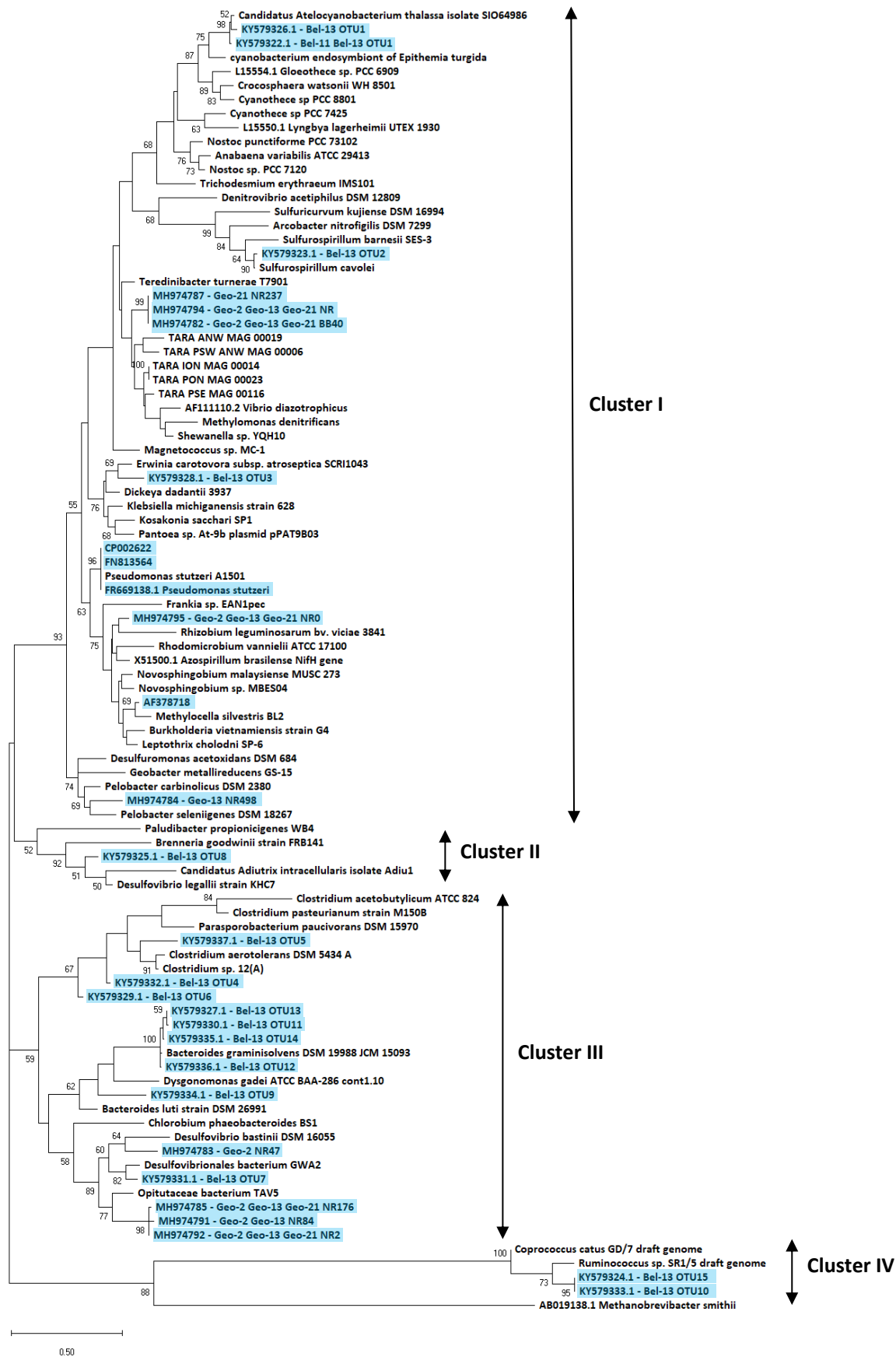
873

874



875

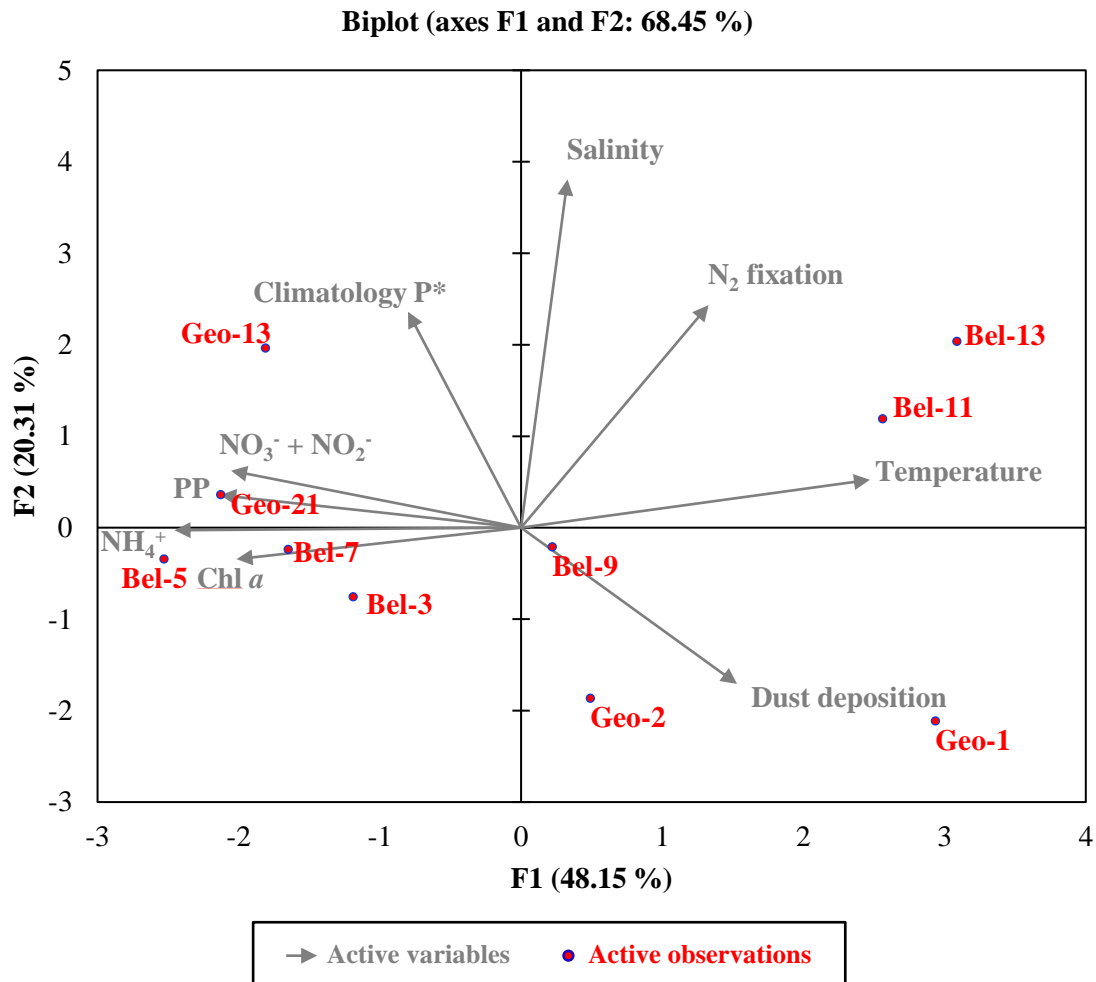
876 **Figure 5:** Diversity of *nifH* sequences during (a) the Belgica BG2014/14 cruise (successfully recovered only at
877 stations Bel-11 and Bel-13, 5 m) and (b) the GEOVIDE cruise (stations Geo-2, 100 m; Geo-13, 35 m and Geo-21, 15
878 and 70 m. The total numbers of recovered sequences are indicated on top of the bars, and the exact percentage
879 represented by each group is shown inside the bars.



880

881 **Figure 6:** Phylogenetic tree of *nifH* predicted amino acid sequences generated using the Maximum Likelihood
 882 method of the Kimura 2-parameter model (Kimura, 1980) via the Molecular Evolutionary Genetics Analysis software

883 (MEGA 7.0) (Kumar et al., 2016). Initial tree(s) for the heuristic search were obtained automatically by applying
884 Neighbor-Join and BioNJ algorithms to a matrix of pairwise distances estimated using the Maximum Composite
885 Likelihood (MCL) approach, and then selecting the topology with superior log likelihood value. A discrete Gamma
886 distribution was used to model evolutionary rate differences among sites (5 categories (+G, parameter = 0.4038)). All
887 sequences recovered from DNA samples, including those previously identified and the newly recovered ones (with \geq
888 95% similarity at the nucleotide level with representative clones) are highlighted in blue. For the *nifH* sequences
889 recovered from the GEOVIDE cruise, only those contributing to the cumulative 98% of recovered sequences were
890 included in this tree. Bootstrap support values ($\geq 50\%$) for 100 replications are shown at nodes. The scale bar
891 indicates the number of sequence substitutions per site. The archaean *Methanobrevibacter smithii* was used as an
892 outgroup. Accession numbers for published sequences used to construct the phylogenetic tree are given.



895

896 **Figure 7:** Euclidean distance biplot illustrating the axis loadings for the two main PCA components based on the
 897 Spearman rank correlation matrix shown in Table S3. Variables taken into account include depth-integrated rates of
 898 N₂ fixation and primary production (PP), average phosphate excess at 20 m depth surrounding each sampled site
 899 recovered from World Ocean Atlas 2013 climatology data between April and June from 1955 to 2012 (Garcia et al.,
 900 2013); satellite average dust deposition (dry + wet) derived during April 2014 (Giovanni online data system, NASA
 901 Goddard Earth Sciences Data and Information Services Center) and ambient variables (temperature, salinity, and
 902 nutrient data). Coloured dots in the biplot represent the projection of the different stations. Axis 1 has high negative
 903 loadings for PP, Chl *a*, NH₄⁺ and NO₃⁻ + NO₂⁻, and high positive loadings for temperature and N₂ fixation rates, with
 904 values of -0.812, -0.768, -0.936, -0.783, 0.942 and 0.506, respectively (see Table S5). Axis 2 has high positive
 905 loadings of 0.584, 0.943 and 0.602 for climatological P*, salinity and N₂ fixation rates, respectively. PCA analysis
 906 was run in XLSTAT 2017 (Addinsoft, Paris, France, 2017).